Supporting Information for

Phenanthroline-Strapped Calix[4]pyrroles. Anion Receptors Displaying Affinity Reversal as a Function of Solvent Polarity

Nam Jung Heo,[a,#] Ju Hyun Oh,[a,#] Jeong Tae Lee,[b] Qing He,[*,c] Jonathan L. Sessler,[*,d] and Sung Kuk Kim[*,a]

[a]*Department of Chemistry and Research Institute of Natural Science, Gyeongsang National University, Jinju 52828, Korea,* [b]*Department of Chemistry and Institute of Applied Chemistry, Hallym University, Chuncheon 24252, Korea,* [c]*State Key Laboratory of Chemo/Biosensing and Chemometrics, College of Chemistry and Chemical Engineering, Hunan University, Changsha 410082, P. R. China, and* [d]*Department of Chemistry, The University of Texas at Austin, 105 E. 24th Street-Stop A5300, Austin, Texas 78712-1224, USA*

1. General experimental and synthetic details

Solvents and reagents used for the synthetic work were purchased from Aldrich, TCI, or Alfa Aesar and used without further purification. Compounds **1** and **4** were prepared as reported previously.[1,2] NMR spectra were recorded on a Bruker Advance-300 MHz instrument. The NMR spectra were referenced to residual solvent peaks and the spectroscopic solvents were purchased from either Cambridge Isotope Laboratories or Aldrich. Chemical ionization (CI) and electrospray ionization (ESI) mass spectra were recorded on a VG ZAB-2E instrument and a VG AutoSpec apparatus, respectively. TLC analyses were carried out using Sorbent Technologies silica gel (200 mm) sheets. Column chromatography was performed on Sorbent silica gel 60 (40–63 mm).

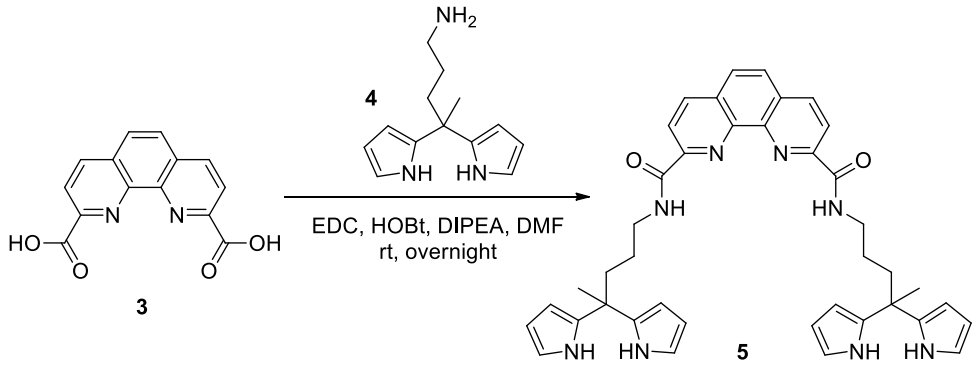

Compound 5: To a solution of compound **3** (0.8 g, 2.98 mmol), compound **4** (1.3 g, 5.98 mmol),[1] EDCI (1-ethyl-3-(3-dimethylaminopropyl)-carbodiimide, 1.02 g, 6.57 mmol) and HOBt (hydroxybenzotriazole, 0.92 g, 6.01 mmol) in DMF (30 mL), DIPEA (N,N-diisopropylethylamine, 2.08 mL, 11.99 mmol) was added via syringe. The resulting solution was stirred overnight at room temperature and concentrated under reduced pressure. To the resulting reaction mass, dichloromethane and water were added. The organic phase was separated off and washed with water. The organic layer was then dried over anhydrous $MgSO_4$ and filtered. The filtrate was evaporated *in vacuo* to give a yellowish sticky solid. Recrystallization of the resulting crude product from acetonitrile gave compound **7** (0.87 g, 44% yield) as a white solid. ^{1}H NMR (300 MHz, $CDCl_3$) δ 8.59 (d, J = 8.3 Hz, 2H), 8.51 (broad t, J = 6.1 Hz, 2H), 8.45 (d, J = 8.3 Hz, 2H), 7.93 (s, 2H), 7.86 (broad s, 4H), 6.59 (t, J = 2.6, 1.7 Hz, 4H), 6.09 (t, J = 2.7 Hz, 8H), 3.50 (q, J = 6.8 Hz, 4H), 2.13 (dd, J = 17.1, 9.1 Hz, 4H), 2.01 (s, 4H), 1.61 (s, 6H) ppm. ^{13}C NMR (75 MHz, DMSO-d_6) δ 164.2, 150.4, 144.2, 138.73, 128.3, 121.6, 116.9, 106.7, 104.1, 79.6, 55.2, 38.7, 25.4 ppm. HRMS (ESI) *m/z* 689.3323 [M + H^+] calc. for $C_{40}H_{42}N_8O_2$, found 689.3324.

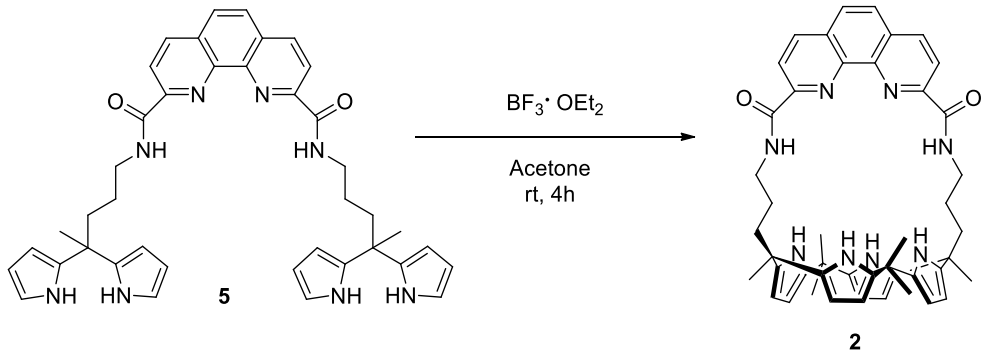

Compound 1: To compound **7** (0.87 g, 1.50 mmol) in acetone (600 ml) was added via syringe BF_3•OEt_2 (boron trifluoride diethyl etherate, 1 mL, 8.10 mmol). The reaction mixture was stirred for 4 hours at room temperature and then quenched with TEA and concentrated under reduced pressure. To this crude product, dichloromethane and water were added. The organic phase was separated off and washed with water. The organic layer was then dried over anhydrous $MgSO_4$, filtered, and evaporated *in vacuo* to give a yellowish solid. The crude product obtained in this way was purified by column chromatography over silica gel (eluent: acetone/dichloromethane (1/9)) to give 0.11 g (11% yield) of **2** as a yellowish solid. ^{1}H NMR (300 MHz, $CDCl_3$) δ 8.68 (d, J = 8.3 Hz, 4H), 8.63 (broad t, J = 6.1 Hz, 2H), 8.50 (d, J = 8.3 Hz, 2H), 7.98 (s, 2H), 7.07 (broad s, 4H), 5.90 (t, J = 3.1 Hz, 4H), 5.82 (t, J = 3.0 Hz, 4H), 3.63 (q, J = 6.4 Hz, 4H), 2.00 (m, 4H), 1.63 (p, 4H), 1.46 (s, 12H), 1.41 (s, 6H) ppm. ^{13}C NMR (75 MHz, DMSO-d_6) δ 164.5, 150.8, 144.6, 138.8, 138.7, 135.9, 128.5, 122.0, 104.2, 103.0, 40.2, 31.3, 30.5, 28.1, 26.6 ppm. HRMS (ESI) *m/z* 747.4129 [M + H^+] calc. for $C_{46}H_{46}N_8O_2$, found 747.4135.

2. ^{1}H NMR spectral data for titrations with anions

a) Treatment used where binding between receptors and anions is governed by a binding/release equilibrium that is slow on the NMR time scale:

Equilibrium: $A + B \underset{}{\overset{K_a}{\rightleftharpoons}} AB$

Equilibrium constant: $K_a = \frac{[AB]}{[A][B]} = \frac{[AB]}{(c(A)-[AB])(c(B)-[AB])}$ (1)

c(A) and c(B) are the initial concentrations of A and B, and [A], [B] and [AB] are the equilibrium concentrations of the three species.

A and B is in slow exchange with the complex AB on the ^{1}H NMR time scale.

Two signals for one specific proton on A can be seen in the spectrum, corresponding to complexed and uncomplexed forms of A:

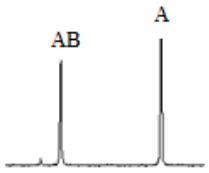

Single-point Methods

K_a is determined from the integrals of complexed and uncomplexed A. If I(A) denotes the integral of a signal for one specific proton of A and I(AB) the integral for the same proton in the complex, the concentration of AB at equilibrium is shown by eq 2. The equilibrium expression is obtrained after substituting into eq. (1):

$$[AB]=\frac{I(AB)}{I(A)+I(AB)}c(A) \quad (2)$$

$$K_a = \frac{I(AB)}{I(A)(c(B)-\frac{I(AB)}{I(A)+I(AB)}c(A))} \quad (3)$$

b) Treatment used where binding between receptors and anions is governed by a binding/release equilibrium that is fast on the NMR time scale:

Binding constants of receptors with anions were calculated using the equation $y = (b \times x)/(1 + x \times Ka)$, where x = [G], y = $|\delta_0 - \delta|$ (δ is the chemical shift of an indicative receptor proton

signal at a certain anion concentration and δ_0 is the chemical shift of the receptor signal for the anion-free form).

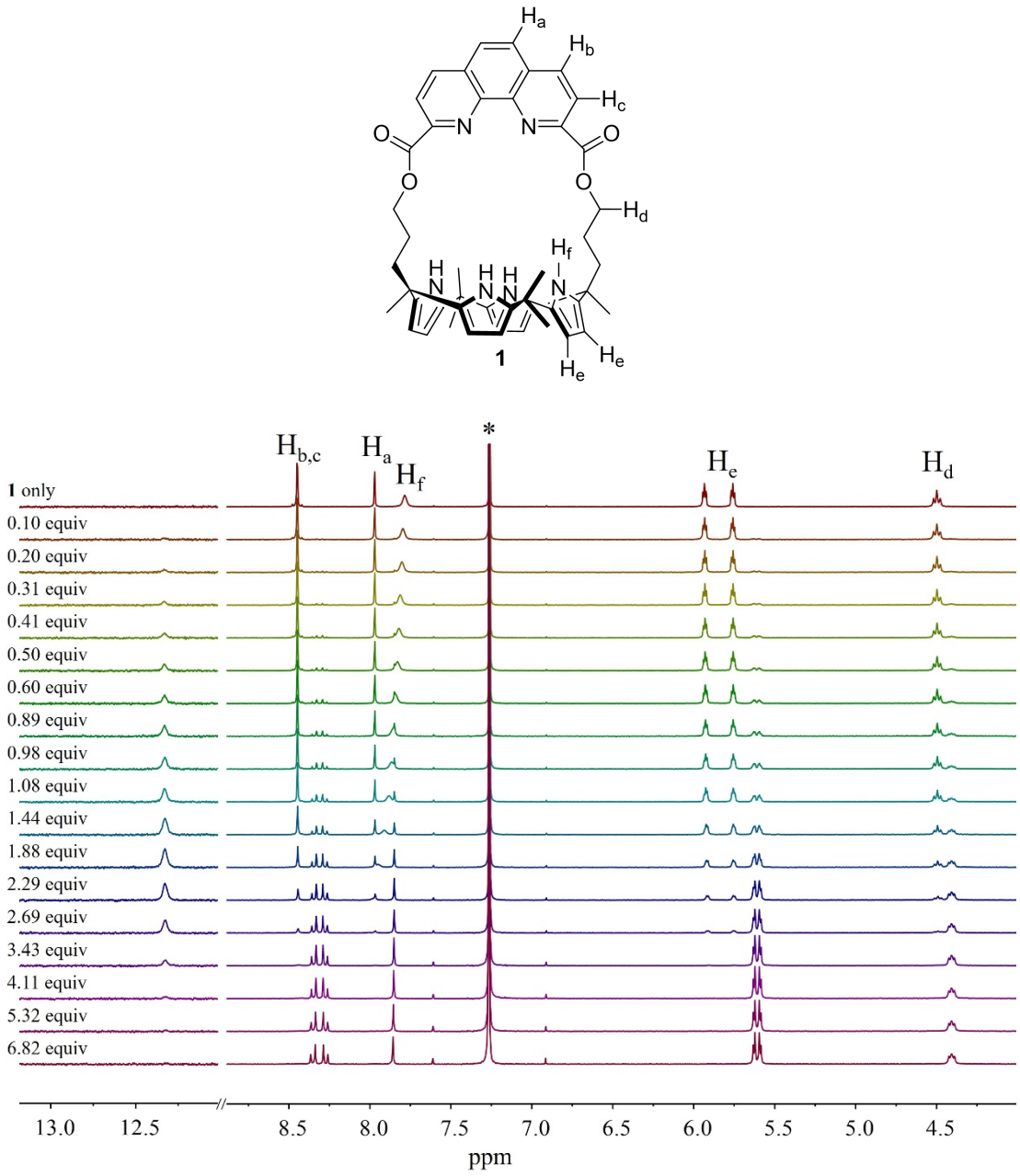

Figure S1. Partial ^{1}H NMR spectra recorded during the titration of **1** (3 mM) with tetraethylammonium bicarbonate ($TEAHCO_3$) in $CDCl_3$.

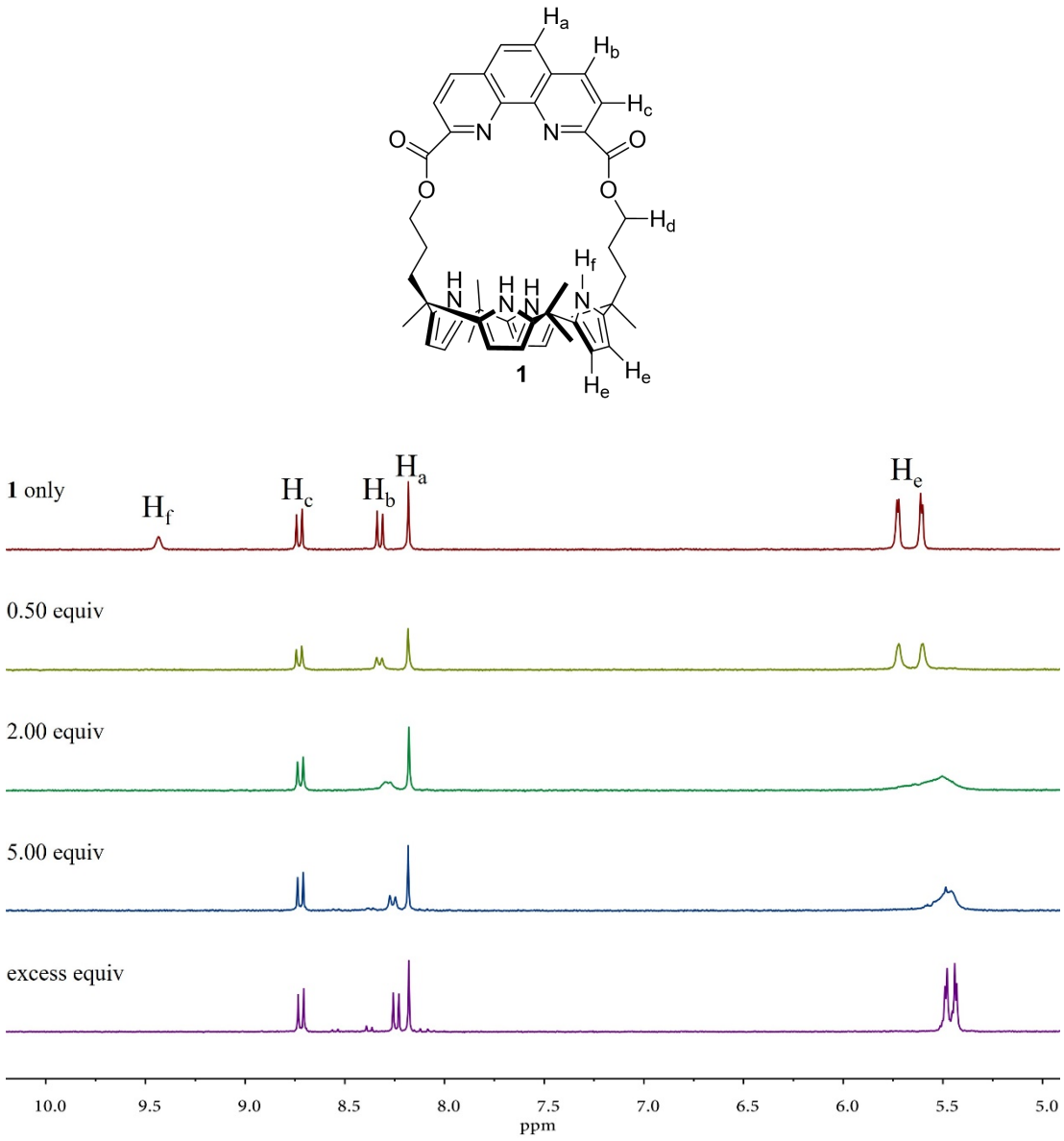

Figure S2. Partial ^{1}H NMR spectra recorded during the titration of **1** (3 mM) with tetraethylammonium bicarbonate ($TEAHCO_3$) in aqueous DMSO-d_6 solution (15% D_2O in DMSO-d_6).

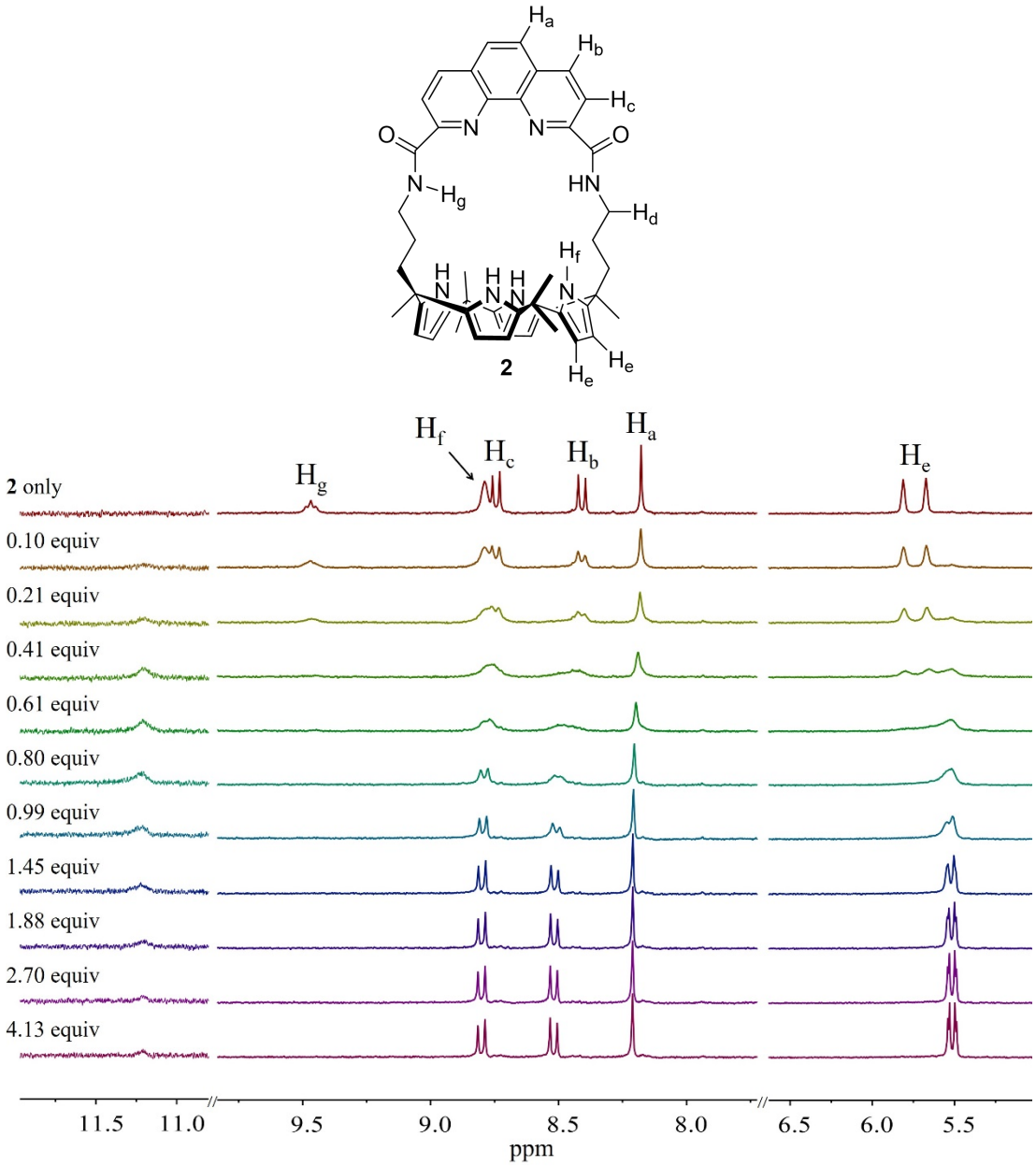

Figure S3. ^{1}H NMR spectra recorded during the titration of **2** (3 mM) with tetraethylammonium bicarbonate ($TEAHCO_3$) in aqueous DMSO-d_6 solution (15% D_2O in DMSO-d_6).

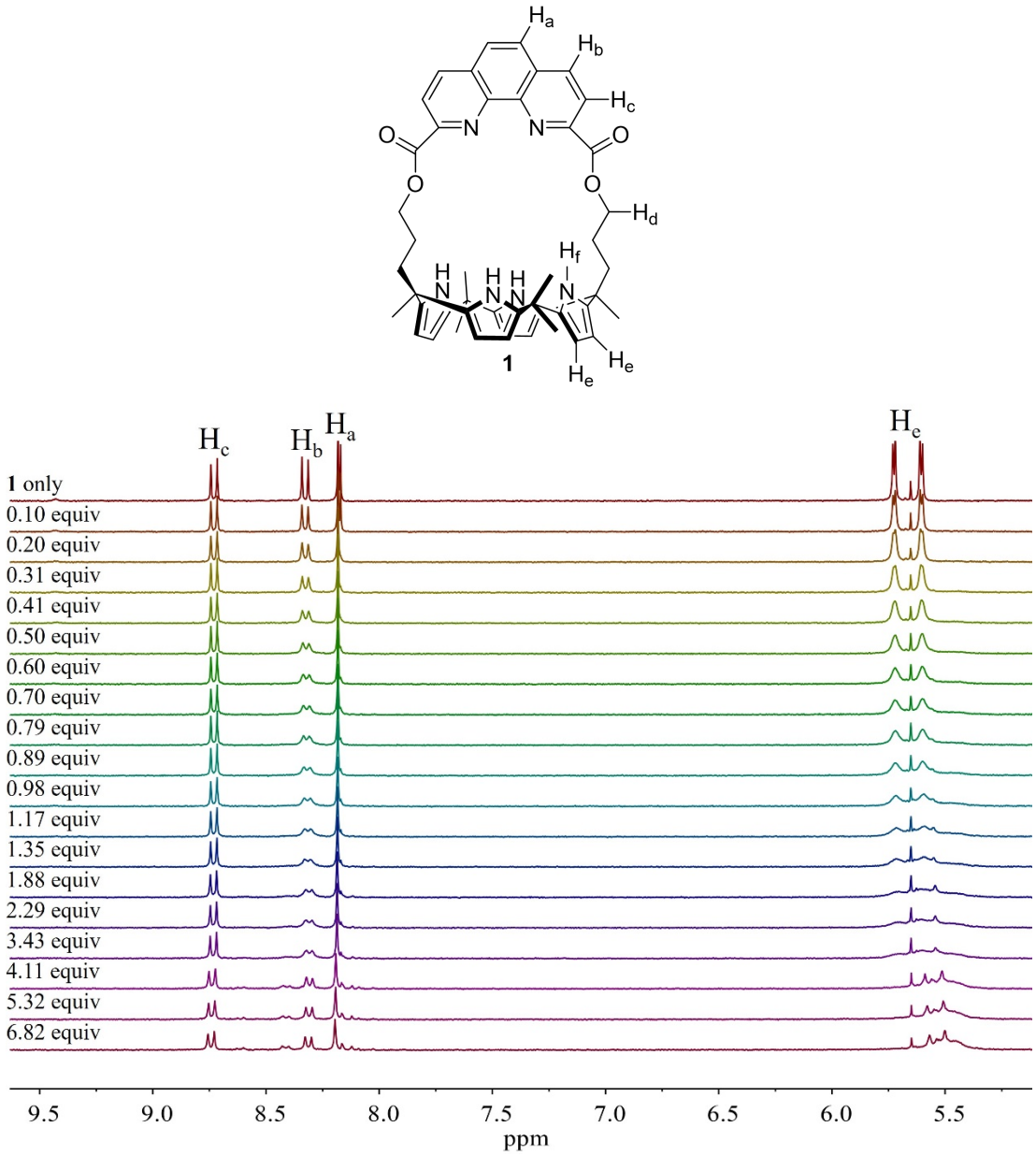

Figure S4. Partial ^{1}H NMR spectra recorded during the titration of **1** (3 mM) with sodium bicarbonate ($NaHCO_3$) in aqueous DMSO-d_6 solution (15% D_2O in DMSO-d_6).

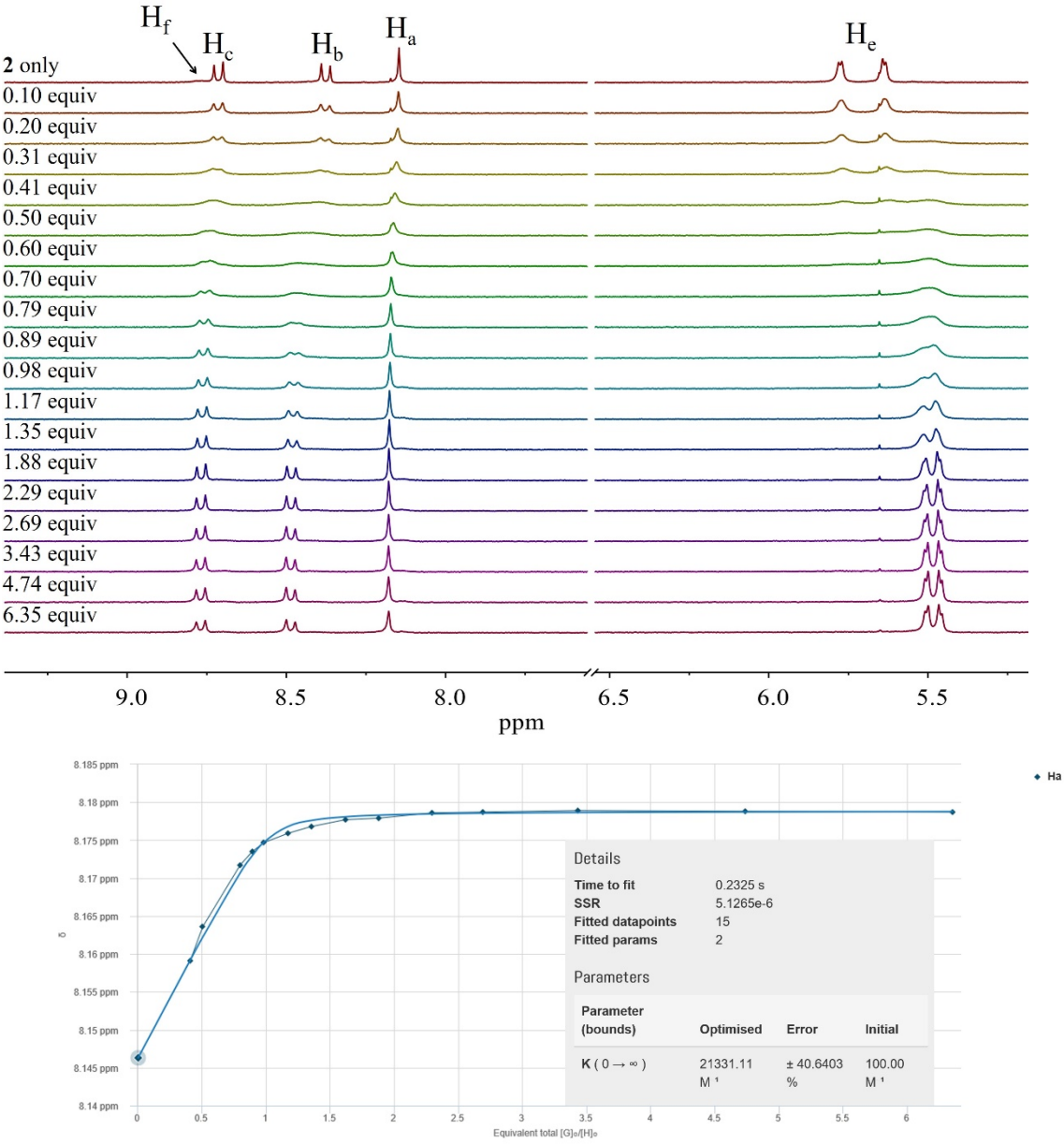

Figure S5. ^{1}H NMR spectra recorded during the titration of **2** (3 mM) with sodium bicarbonate ($NaHCO_3$) in aqueous DMSO-d_6 solution (15% D_2O in DMSO-d_6) and the corresponding isotherm for the binding of $NaHCO_3$ obtained using BindFit v5.0 available from URL: "http://app.supramolecular.org/bindfit/". The data was fitted based on the chemical shift changes of the signal corresponding to H_a.

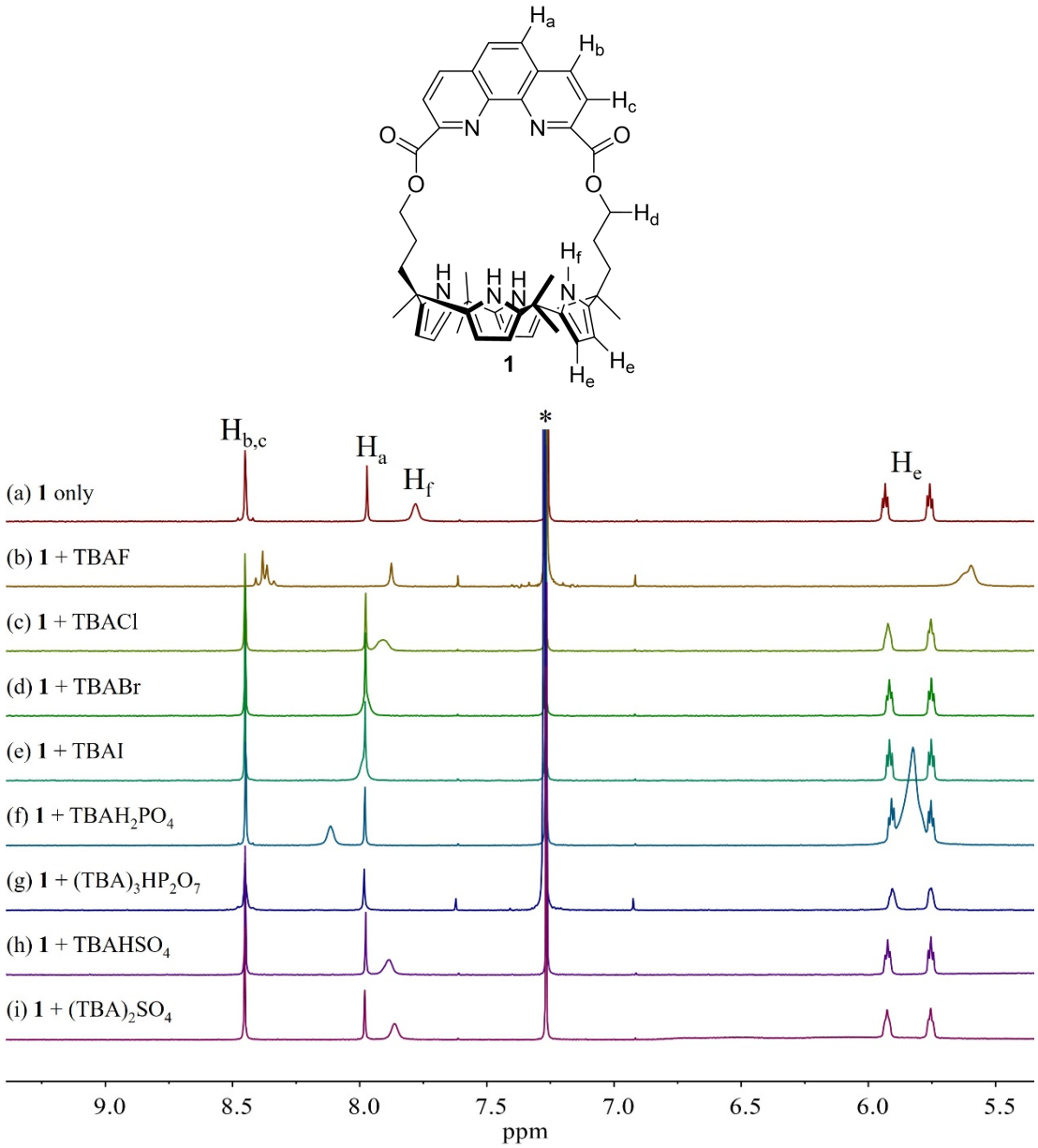

Figure S6. Partial 1H NMR spectra of (a) **1** (3 mM) only, (b) **1** + excess TBAF (tetrabutylammonium fluoride), (c) **1** + excess TBACl, (d) **1** + excess TBABr, (e) **1** + excess TBAI, (f) **1** + excess $TBAH_2PO_4$, (g) **1** + excess $(TBA)_3HP_2O_7$, (h) **1** + excess $TBAHSO_4$, and (i) **1** + excess $(TBA)_2SO_4$ in $CDCl_3$.

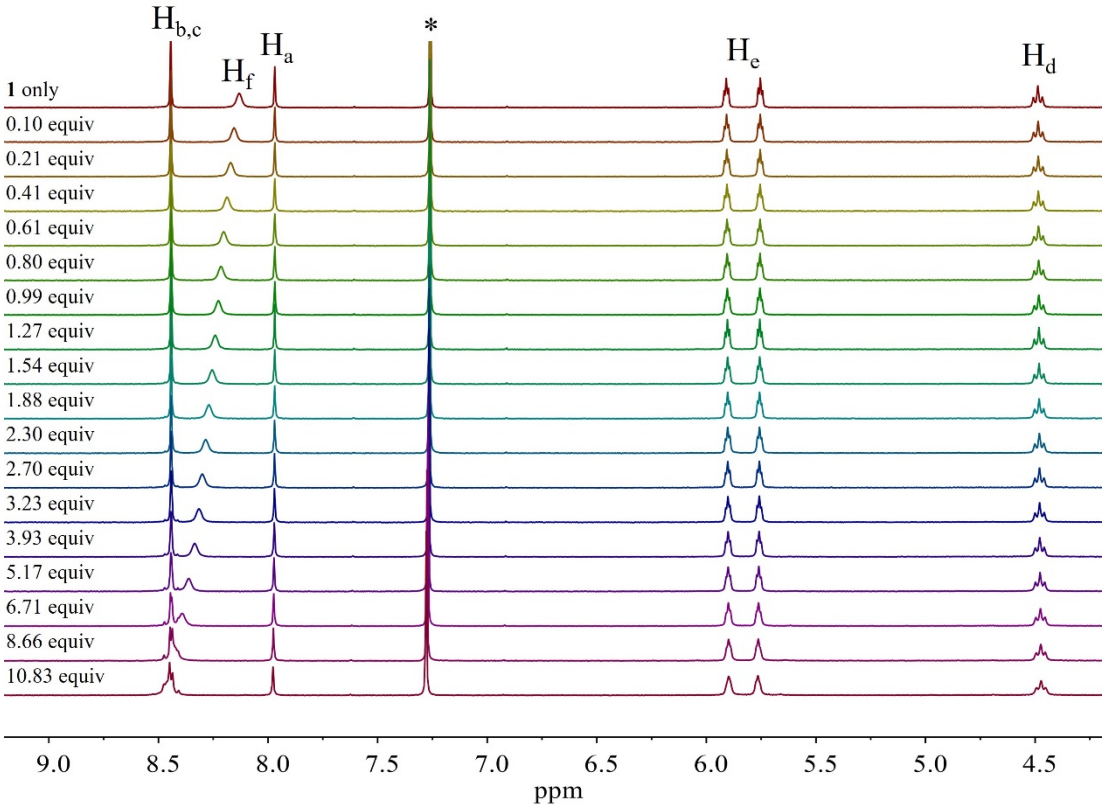

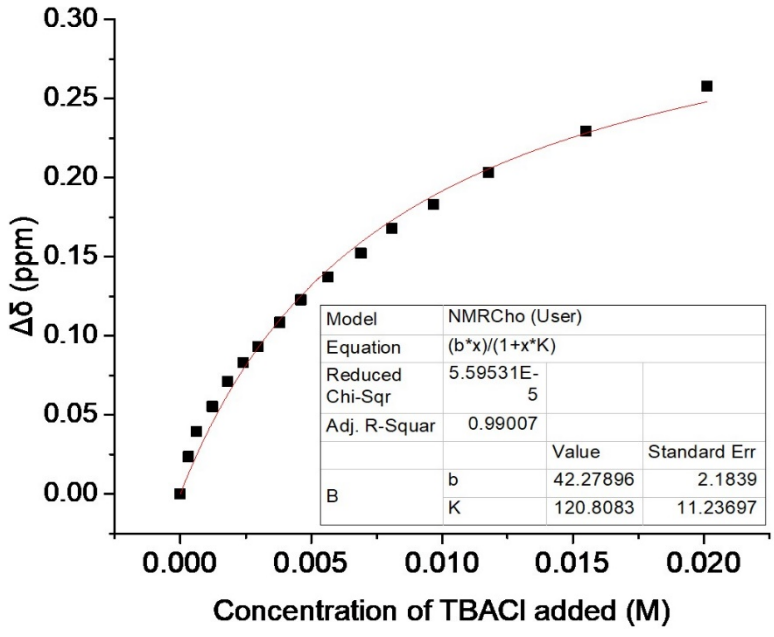

Figure S7. Partial ^{1}H NMR spectra recorded during the titration of **1** (3 mM) with TBACl in $CDCl_3$ and the corresponding binding isotherm. The data was fitted based on the chemical shift changes of the signal corresponding to H_f.

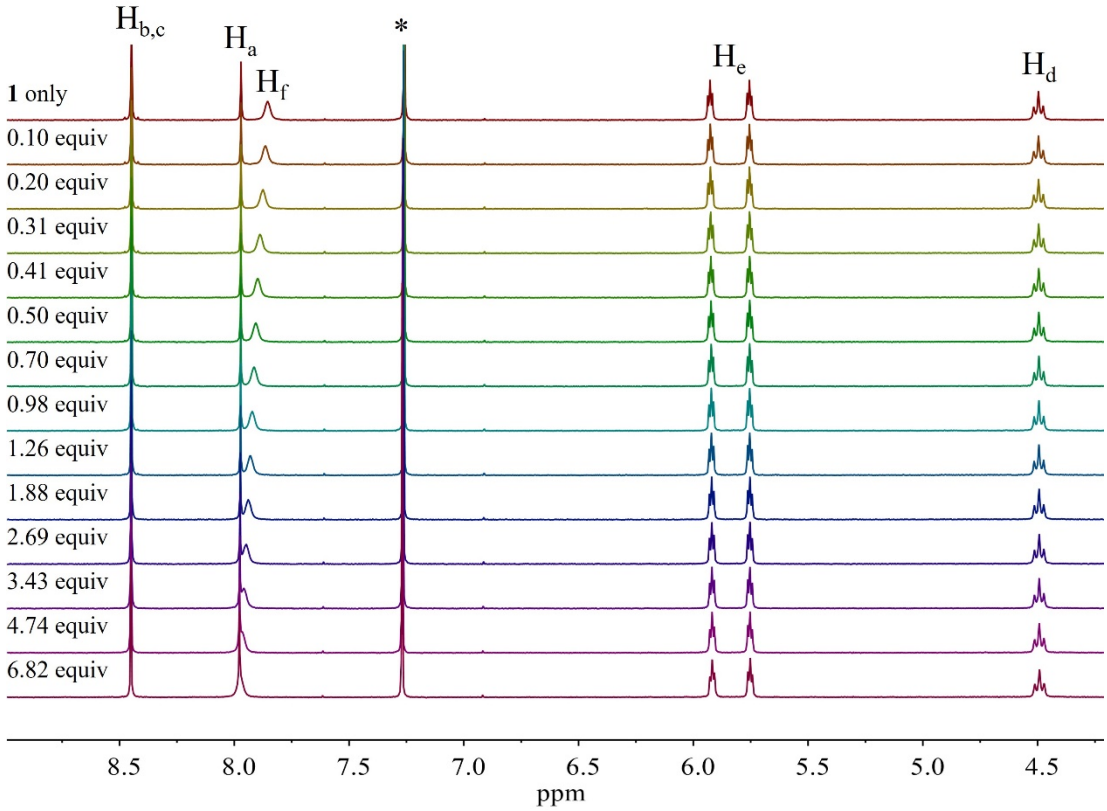

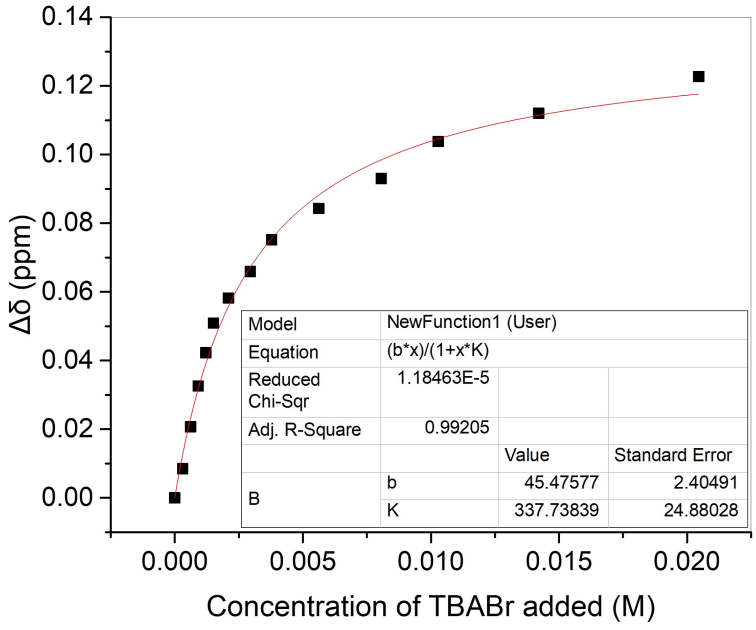

Figure S8. Partial ^{1}H NMR spectra recorded during the titration of **1** (3 mM) with TBABr in $CDCl_3$ and the corresponding binding isotherm. The data was fitted based on the chemical shift changes of the signal corresponding to H_f.

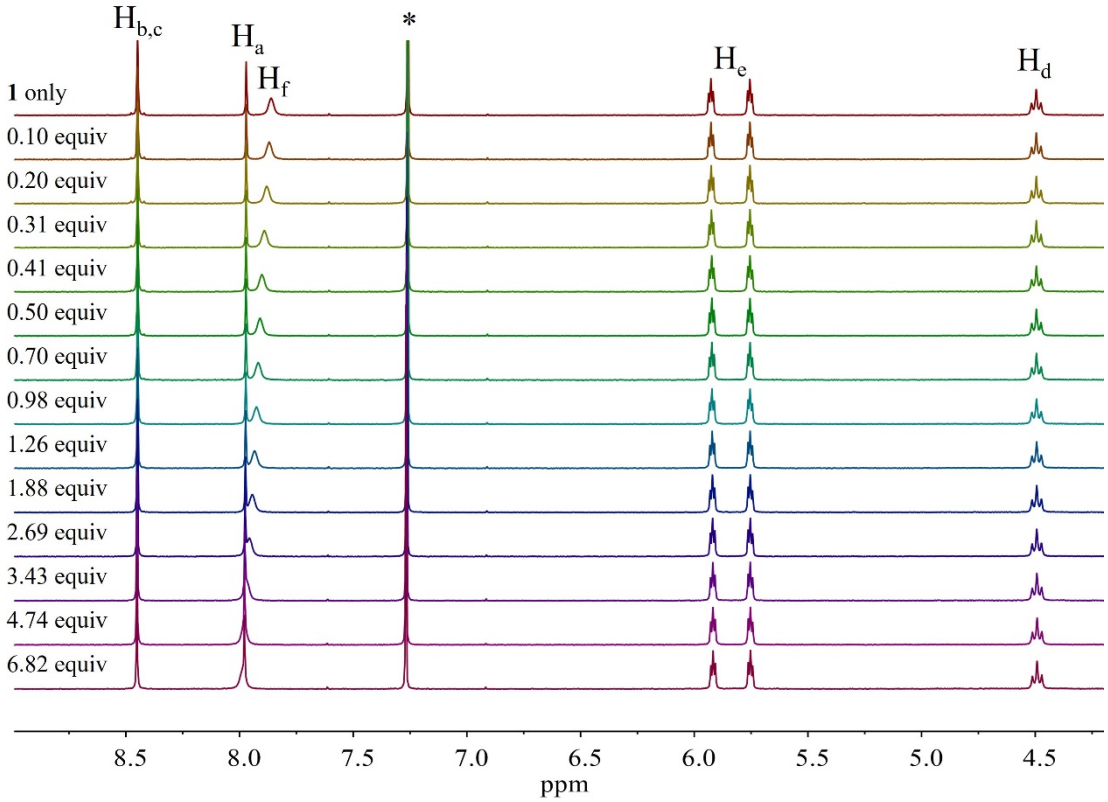

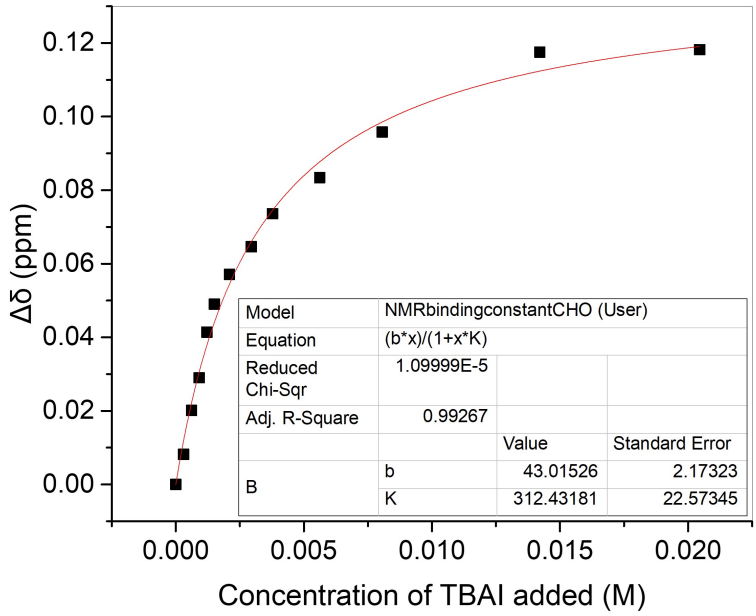

Figure S9. Partial ^{1}H NMR spectra recorded during the titration of **1** (3 mM) with TBAI in $CDCl_3$ and the corresponding binding isotherm. The data was fitted based on the chemical shift changes of the signal corresponding to H_f.

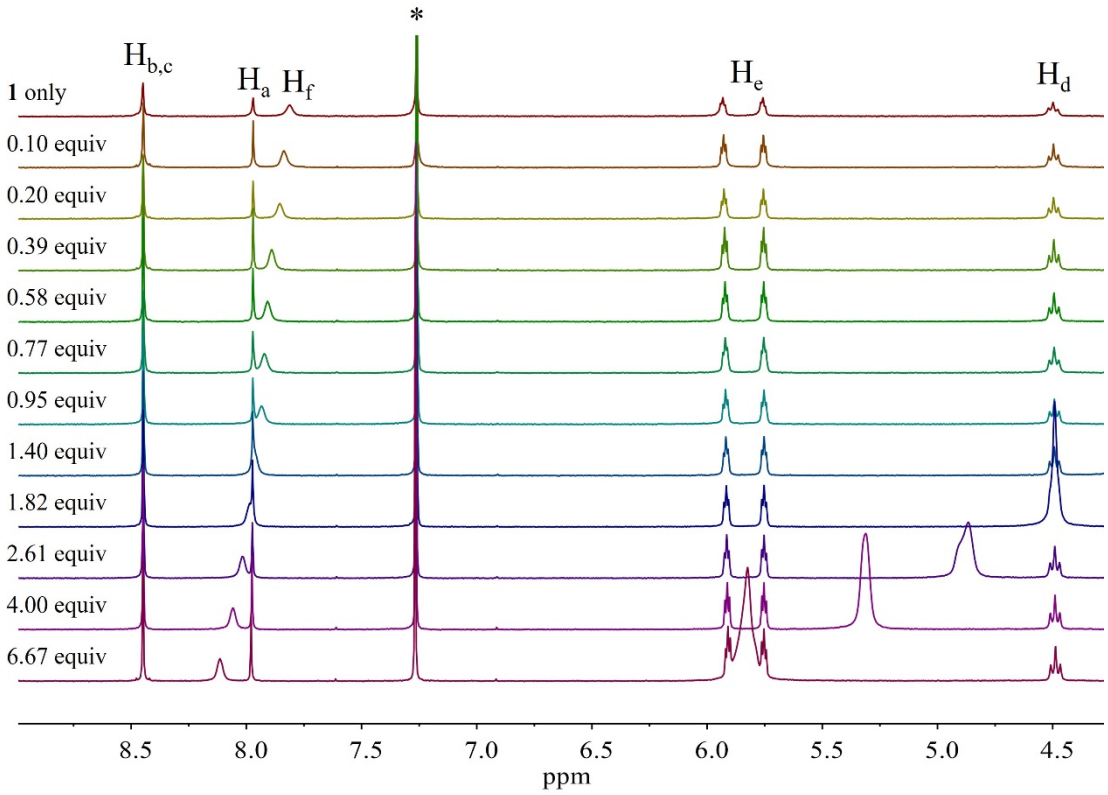

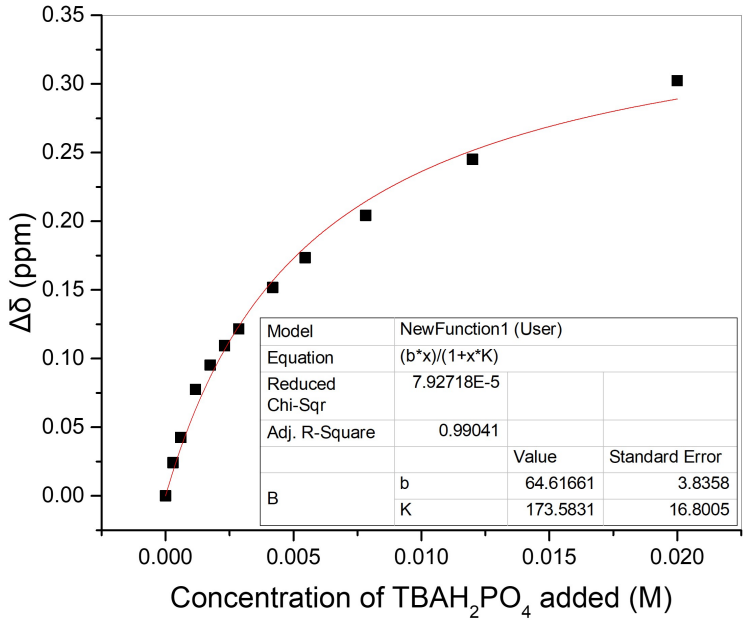

Figure S10. Partial ^{1}H NMR spectra recorded during the titration of **1** (3 mM) with $TBAH_2PO_4$ in $CDCl_3$ and the corresponding binding isotherm. The data was fitted based on the chemical shift changes of the signal corresponding to H_f.

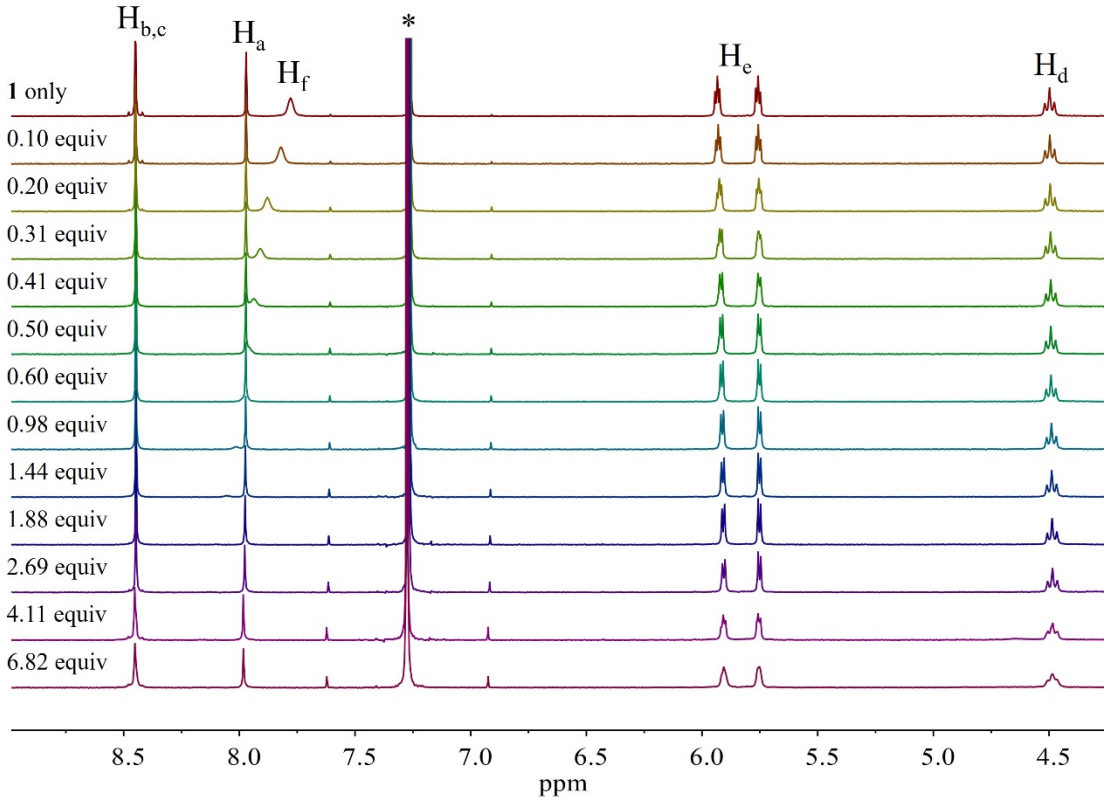

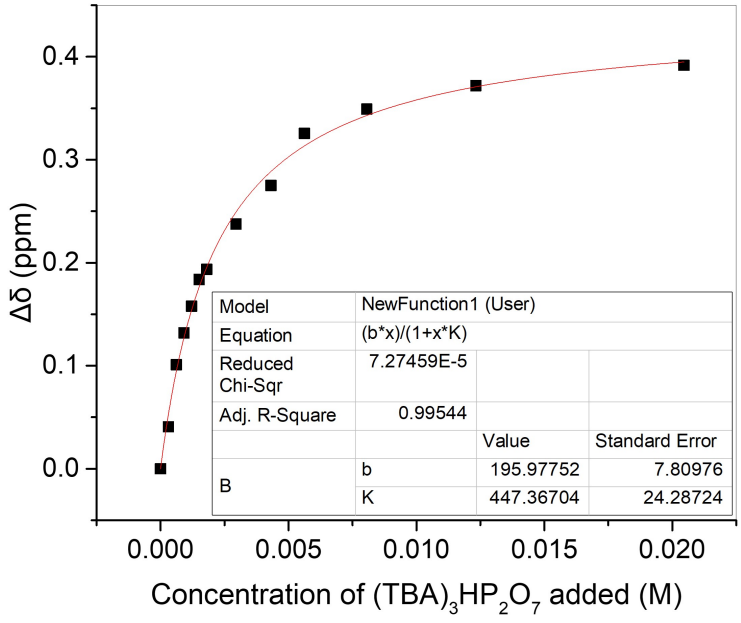

Figure S11. Partial ^{1}H NMR spectra recorded during the titration of **1** (3 mM) with $(TBA)_3HP_2O_7$ in $CDCl_3$ and the corresponding binding isotherm. The data was fitted based on the chemical shift changes of the signal corresponding to H_f.

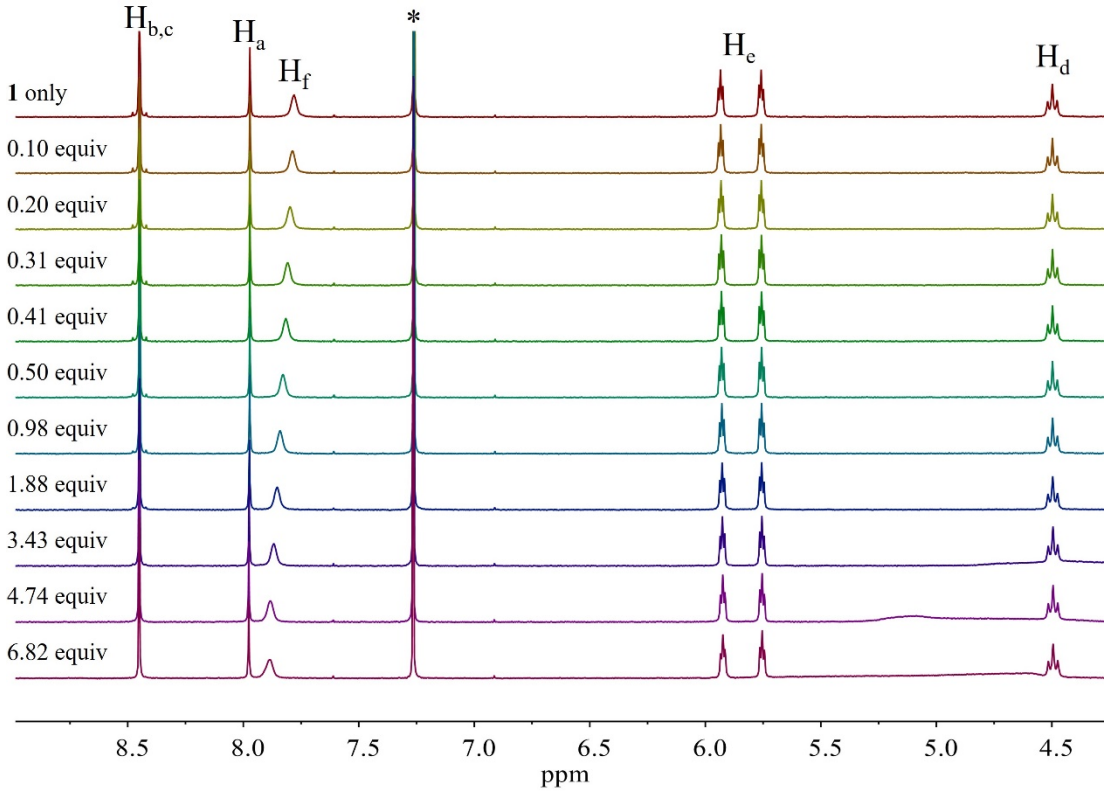

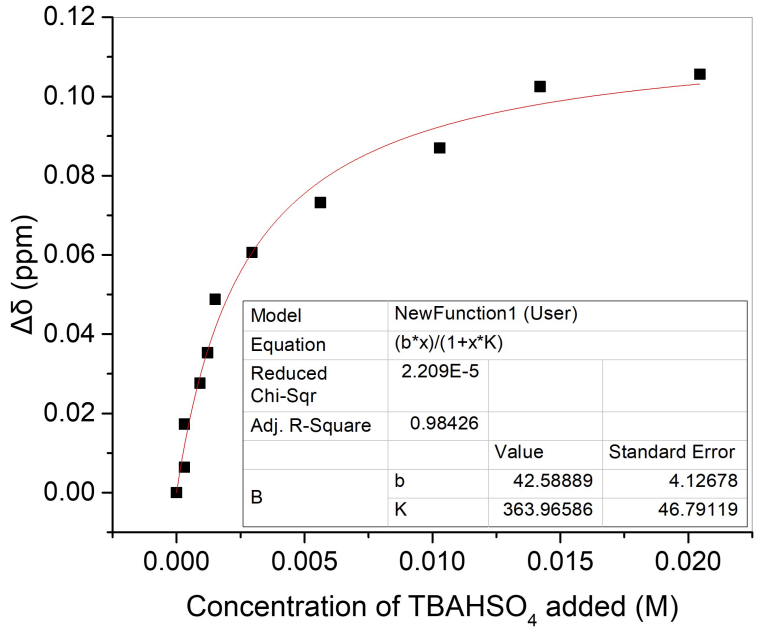

Figure S12. Partial ^{1}H NMR spectra recorded during the titration of **1** (3 mM) with tetrabutylammonium hydrogen sulfate ($TBAHSO_4$) in $CDCl_3$, and the corresponding binding isotherm, which yields. The data was fitted based on the chemical shift changes of the signal corresponding to H_f.

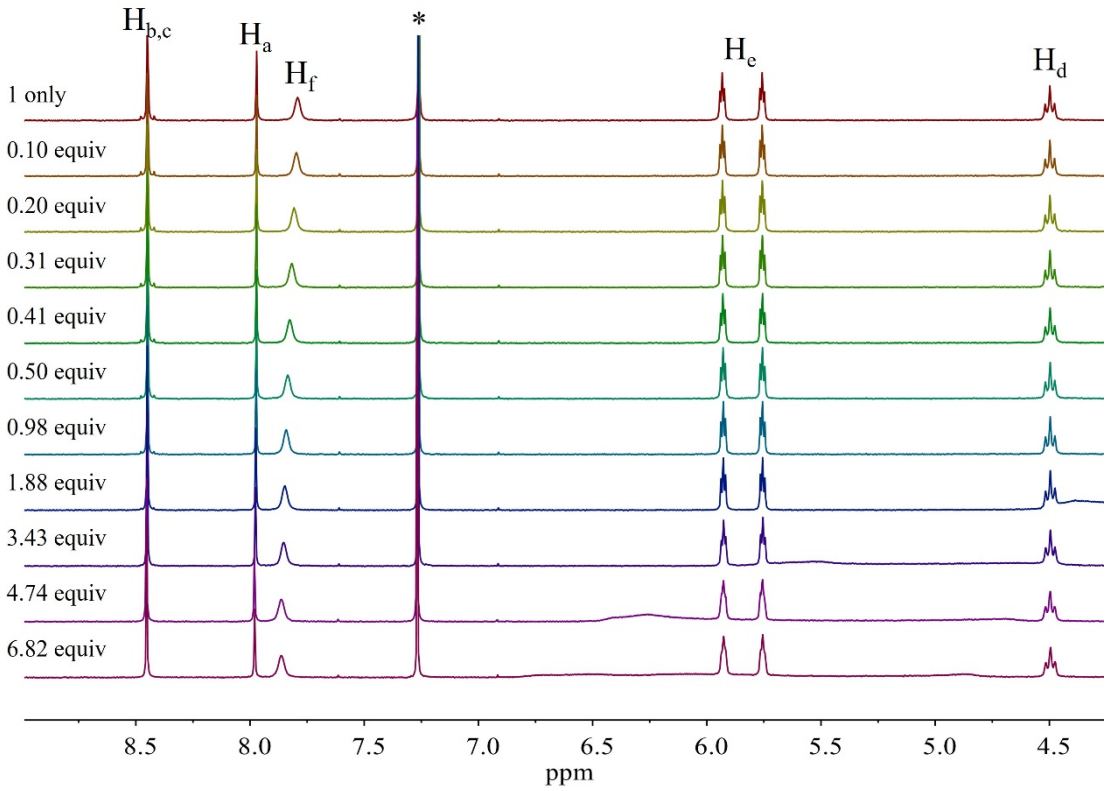

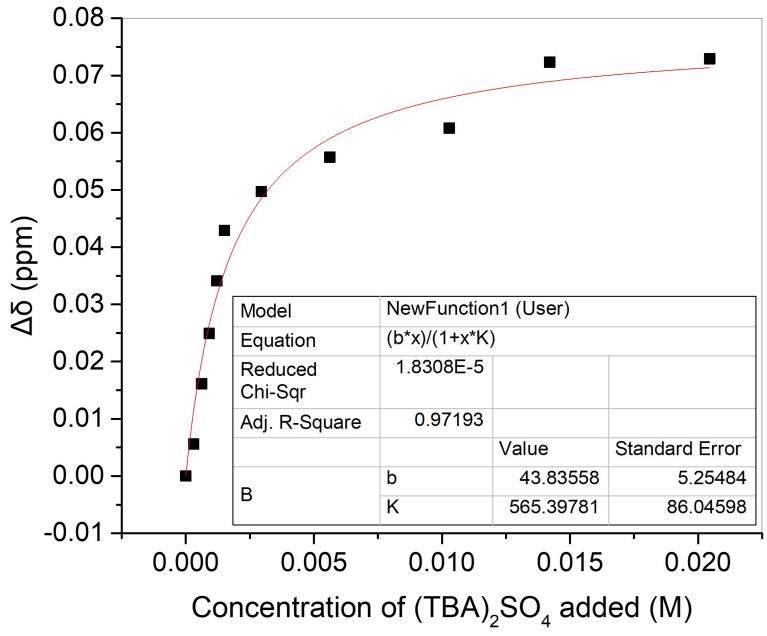

Figure S13. ^{1}H NMR spectra recorded during the titration of **1** (3 mM) with $(TBA)_2SO_4$ in $CDCl_3$ and the corresponding binding isotherm. The data was fitted based on the chemical shift changes of the signal corresponding to H_f.

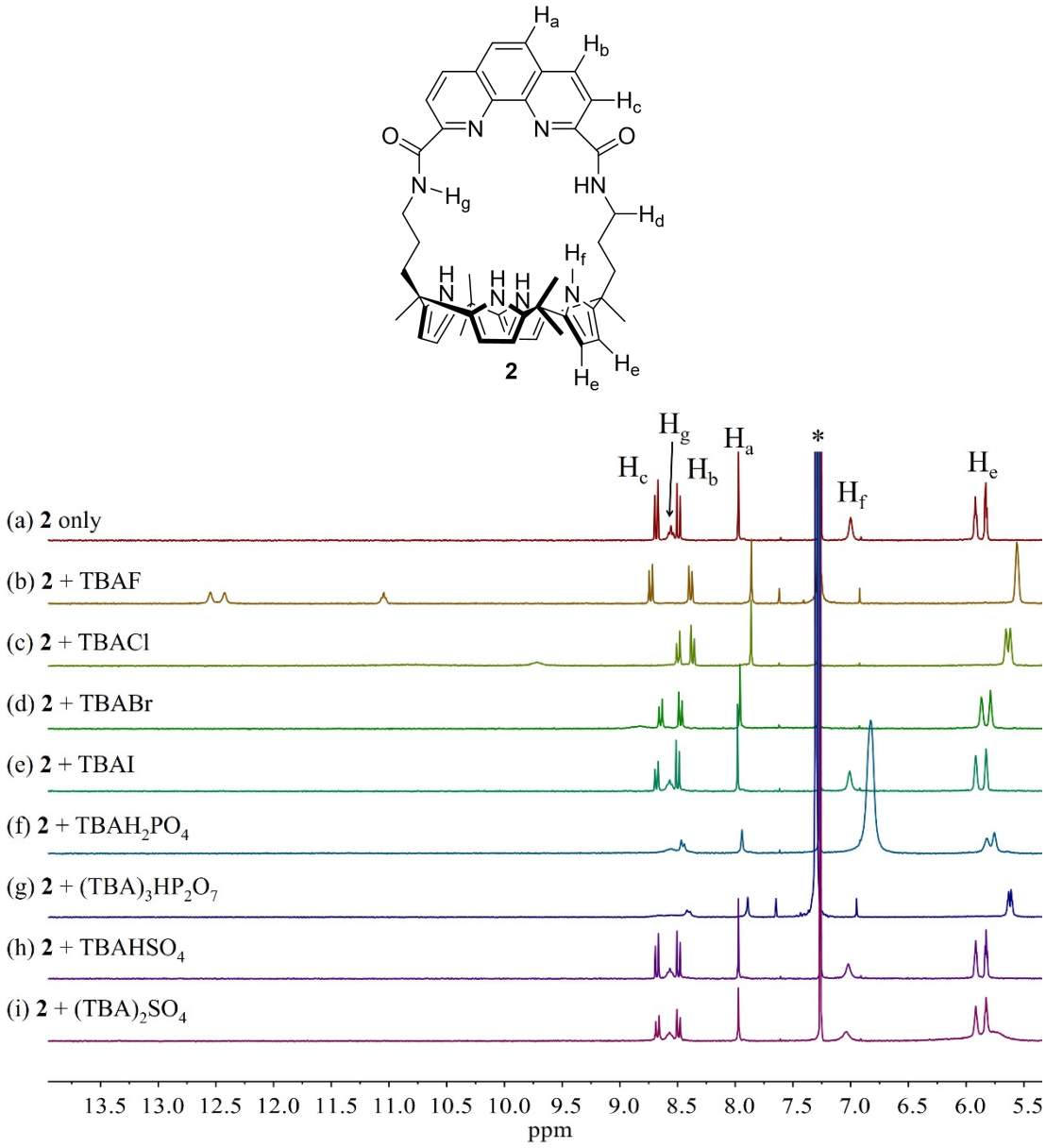

Figure S14. Partial ^{1}H NMR spectra of (a) **2** (3 mM) only, (b) **2** + excess TBAF (tetrabutylammonium fluoride), (c) **2** + excess TBACl, (d) **2** + excess TBABr, (e) **2** + excess TBAI, (f) **2** + excess $TBAH_2PO_4$, (g) **2** + excess $(TBA)_3HP_2O_7$, (h) **2** + excess $TBAHSO_4$, and (i) **2** + excess $(TBA)_2SO_4$ in $CDCl_3$.

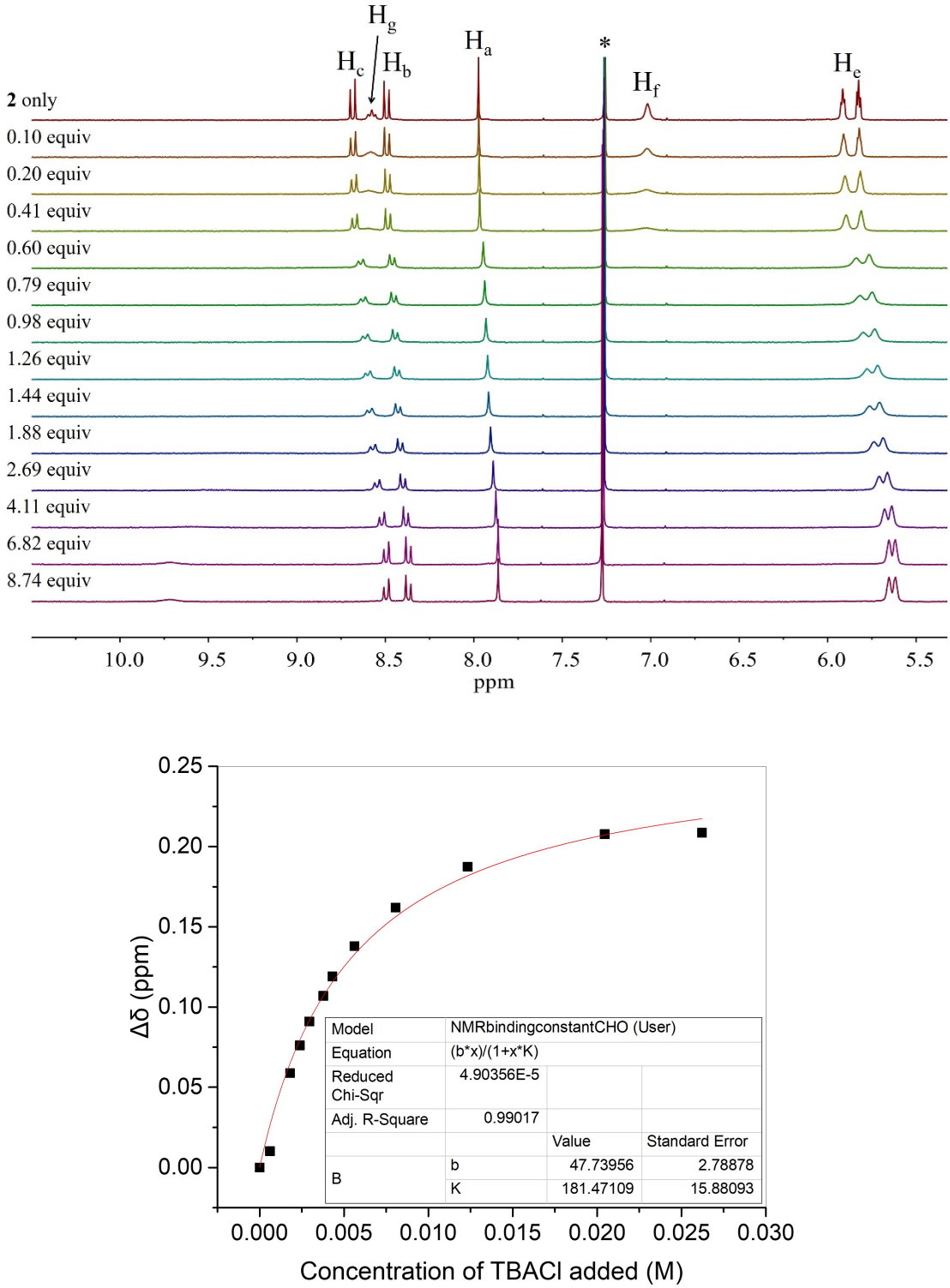

Figure S15. Partial ^{1}H NMR spectra recorded during the titration of **2** (3 mM) with TBACl in $CDCl_3$ and the corresponding binding isotherm for TBACl. The data was fitted based on the chemical shift changes of the signal corresponding to H_e.

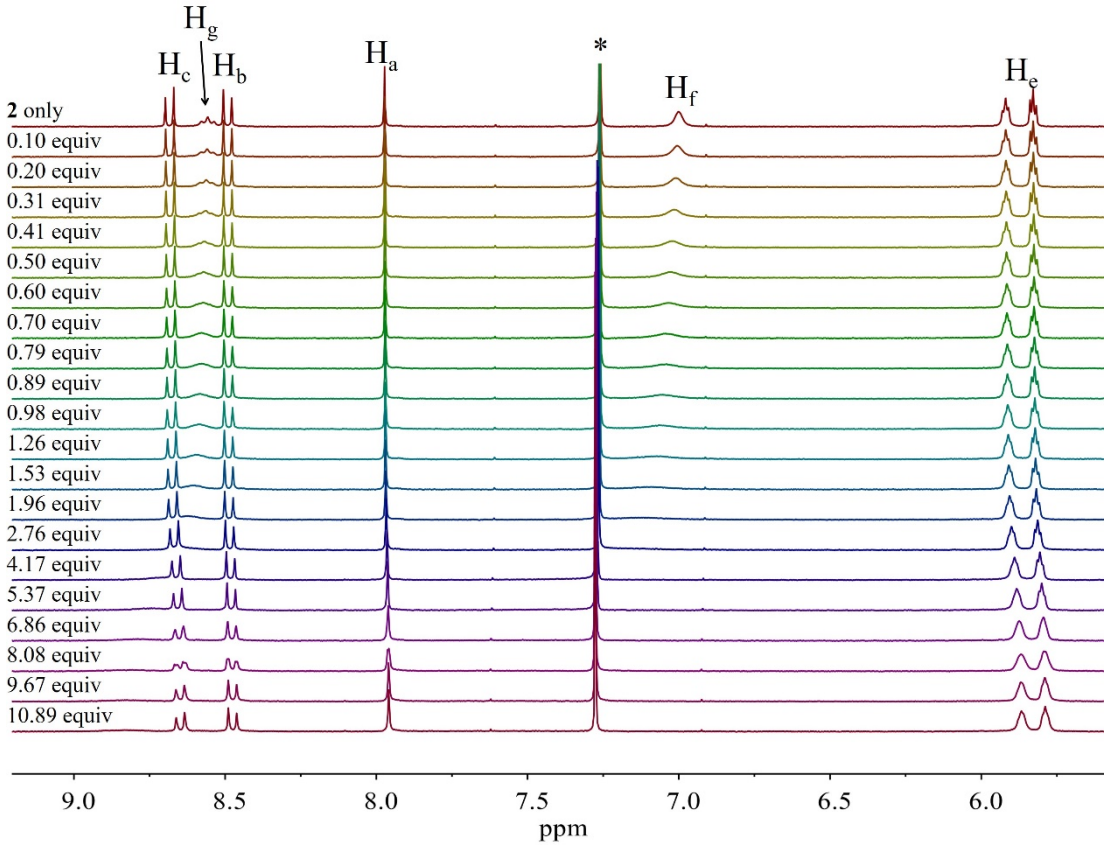

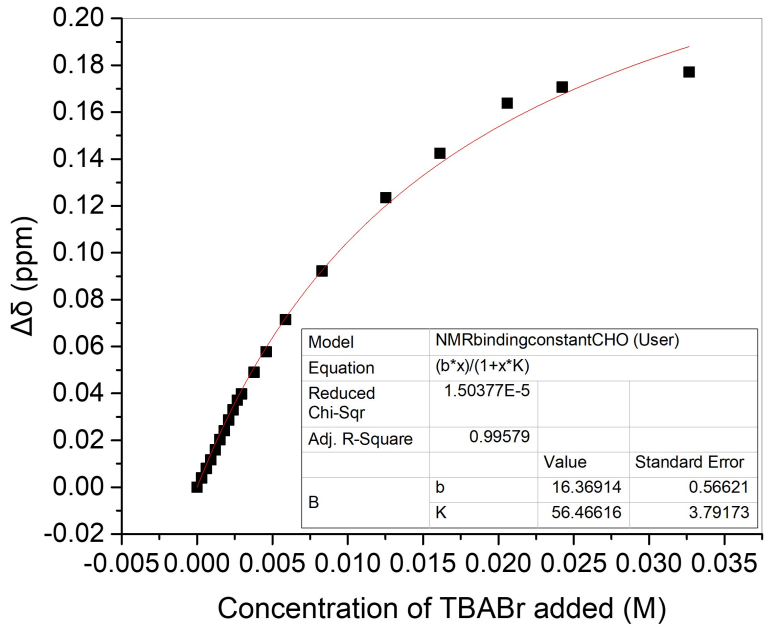

Figure S16. Partial ^{1}H NMR spectra recorded during the titration of **2** (3 mM) with TBABr in $CDCl_3$ and the corresponding binding isotherm. The data was fitted based on the chemical shift changes of the signal corresponding to the methyl protons on the calix[4]pyrrole framework.

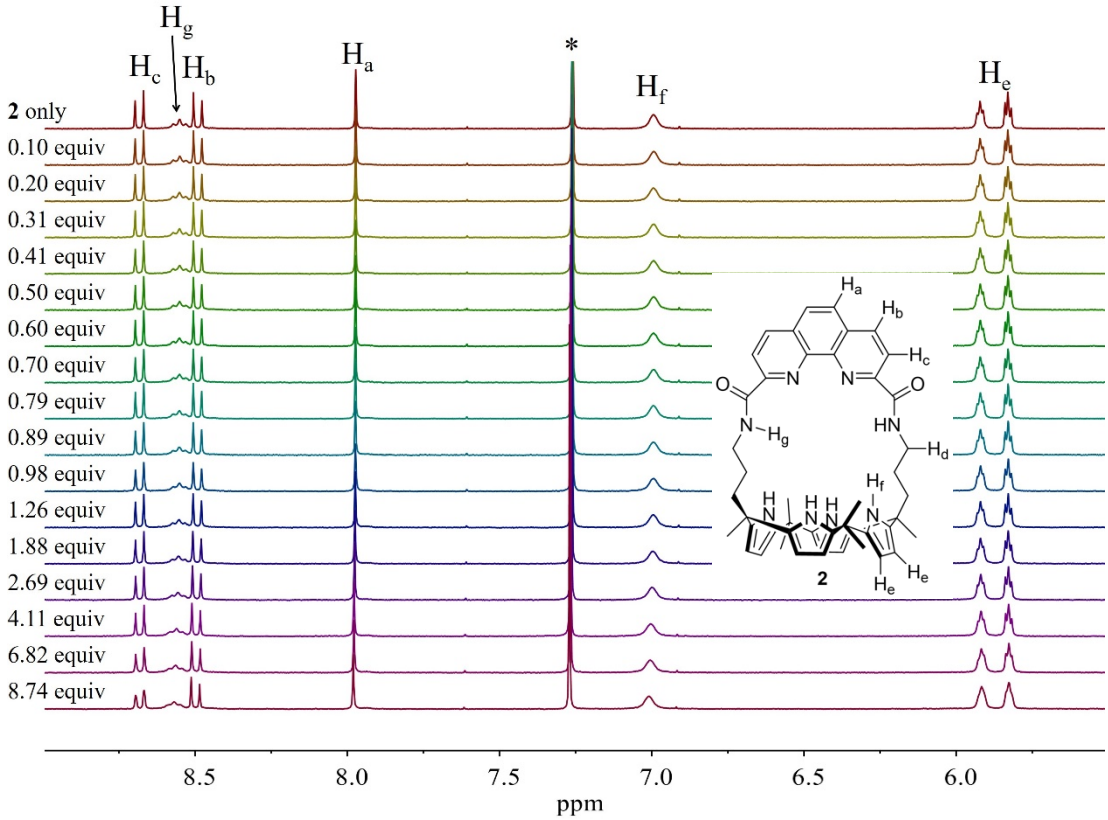

Figure S17. Partial ^{1}H NMR spectra recorded during the titration of **2** (3 mM) with TBAI in $CDCl_3$.

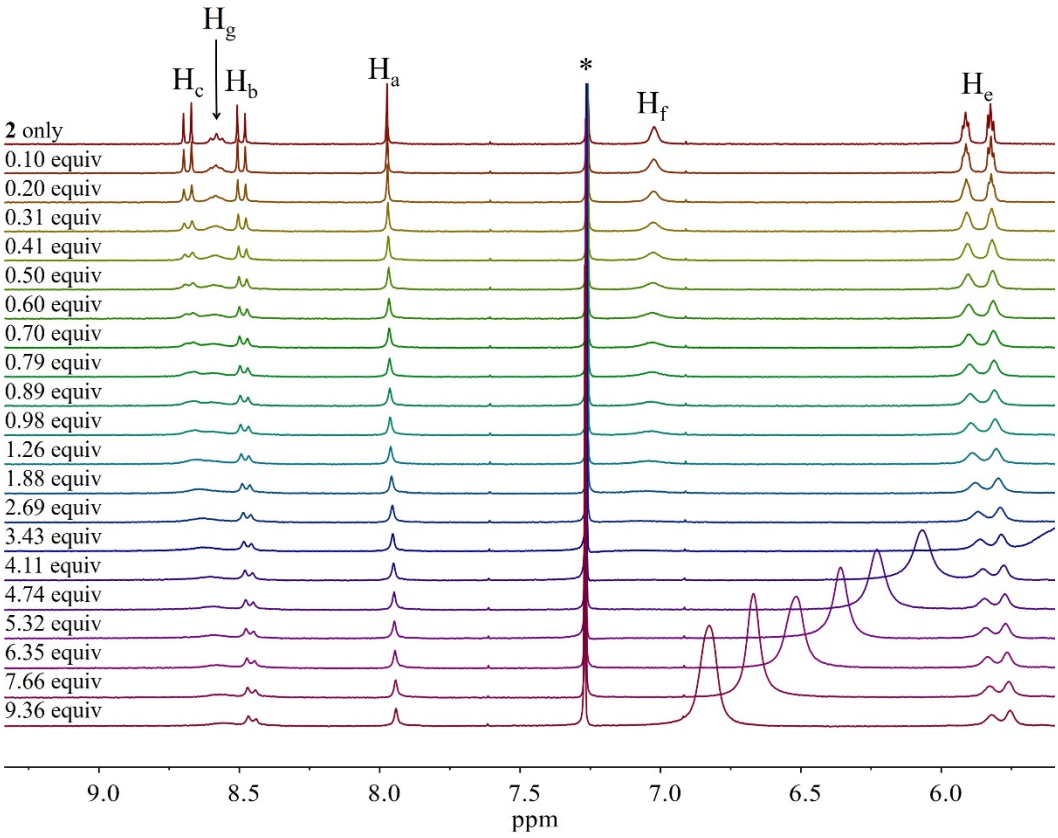

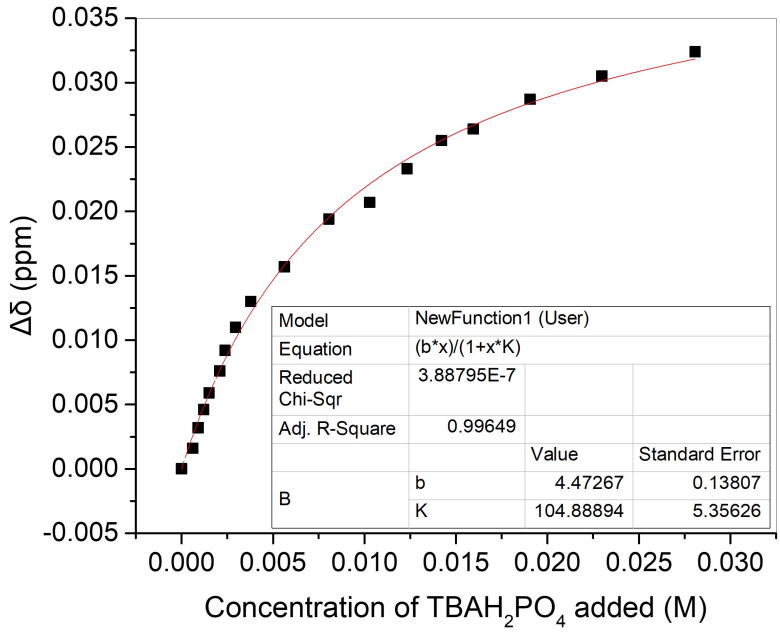

Figure S18. Partial ^{1}H NMR spectra recorded during the titration of **2** (3 mM) with $TBAH_2PO_4$ in $CDCl_3$ and the corresponding binding isotherm. The data was fitted based on the chemical shift changes of the signal corresponding to H_a.

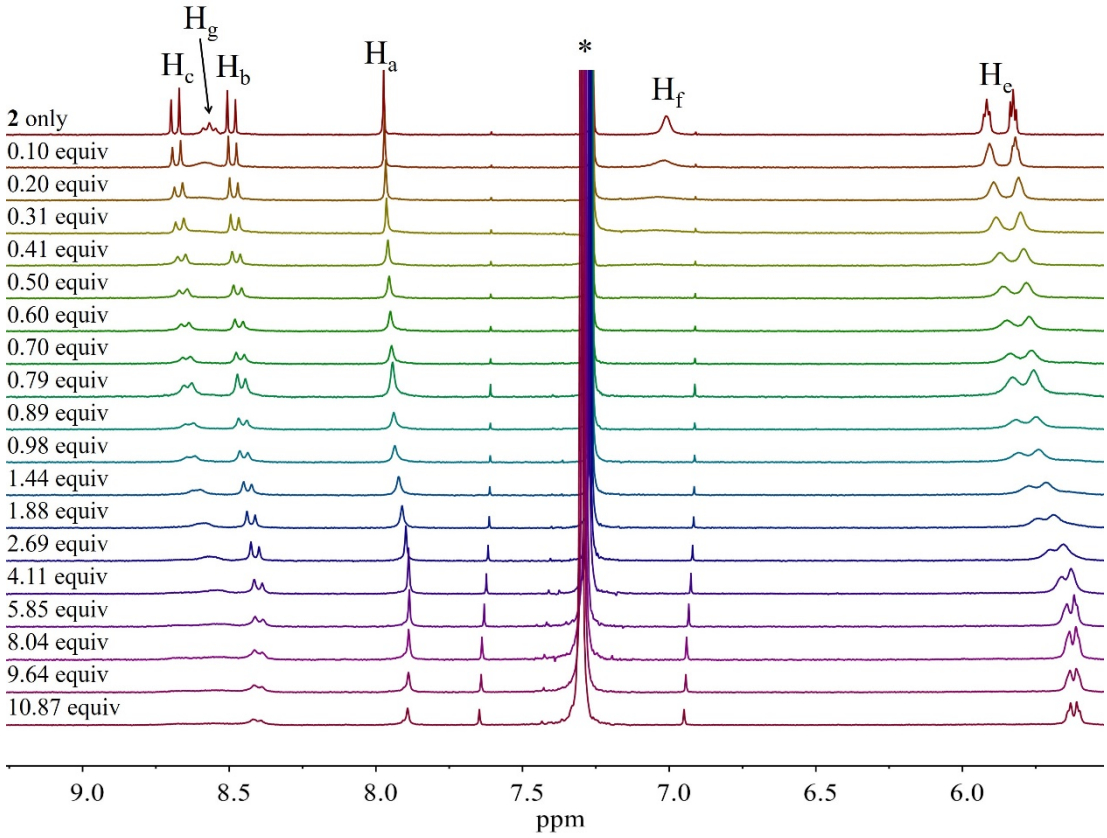

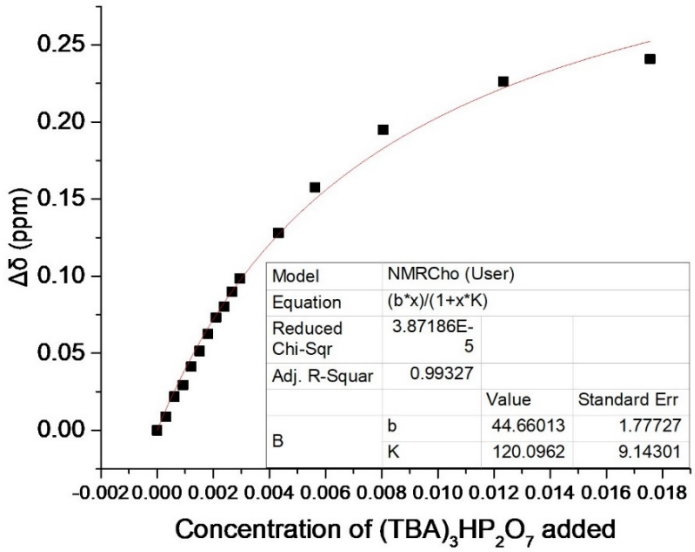

Figure S19. Partial ^{1}H NMR spectra recorded during the titration of **2** (3 mM) with $(TBA)_3HP_2O_7$ in $CDCl_3$ and the corresponding binding isotherm. The data was fitted based on the chemical shift changes of the signal corresponding to H_a.

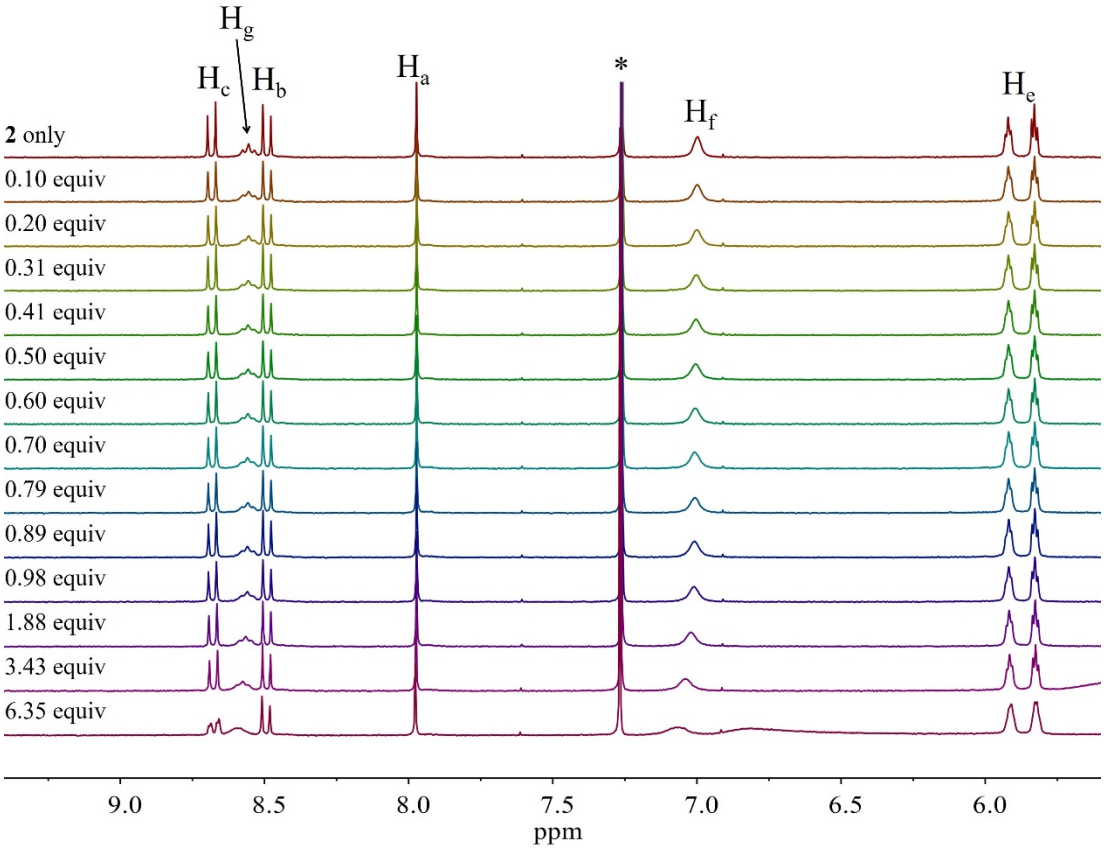

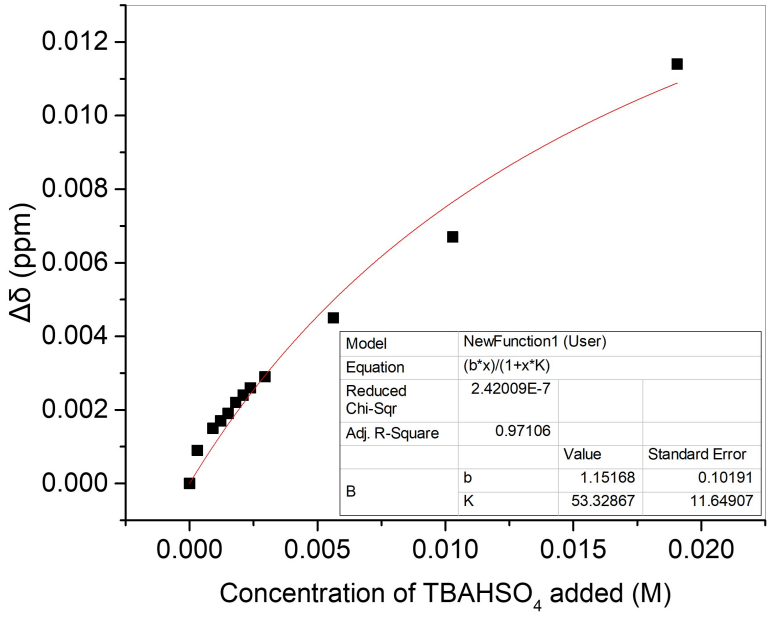

Figure S20. Partial ^{1}H NMR spectra recorded during the titration of **2** (3 mM) with $TBAHSO_4$ in $CDCl_3$ and the corresponding binding isotherm. The data was fitted based on the chemical shift changes of the signal corresponding to H_c.

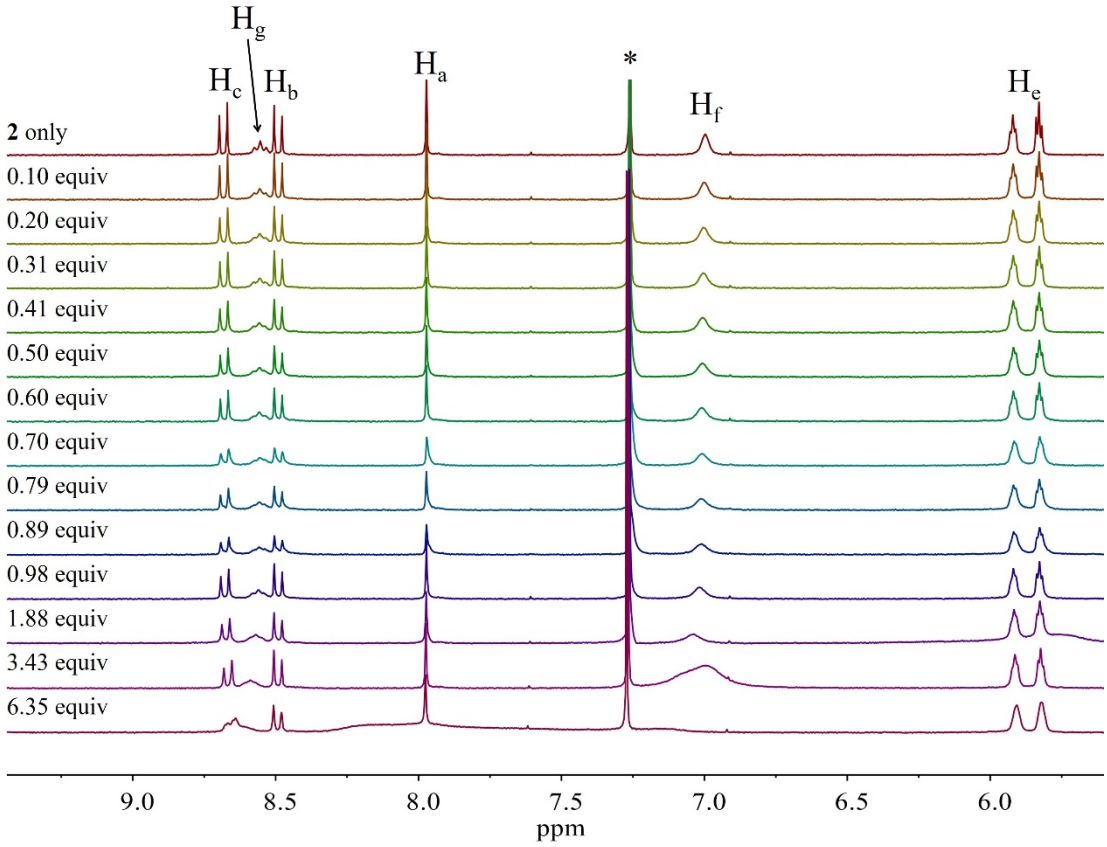

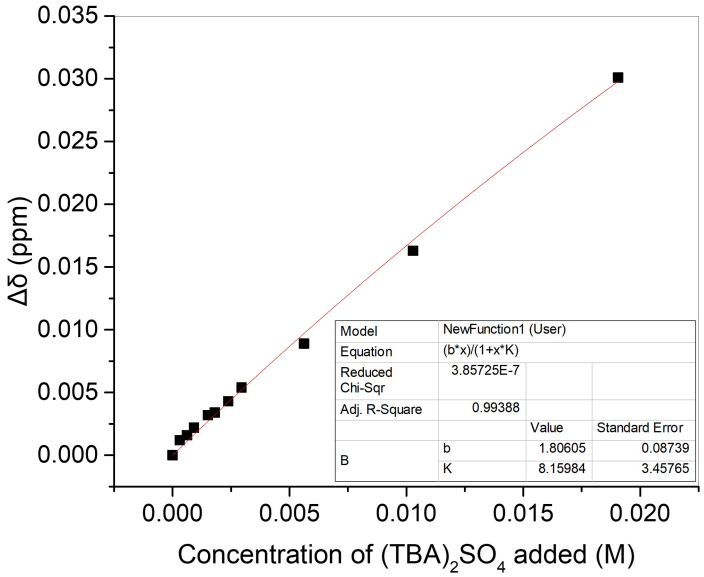

Figure S21. ^{1}H NMR spectra recorded during the titration of **2** (3 mM) with $(TBA)_2SO_4$ in $CDCl_3$ and the corresponding binding isotherm. The data was fitted based on the chemical shift changes of the signal corresponding to H_c.

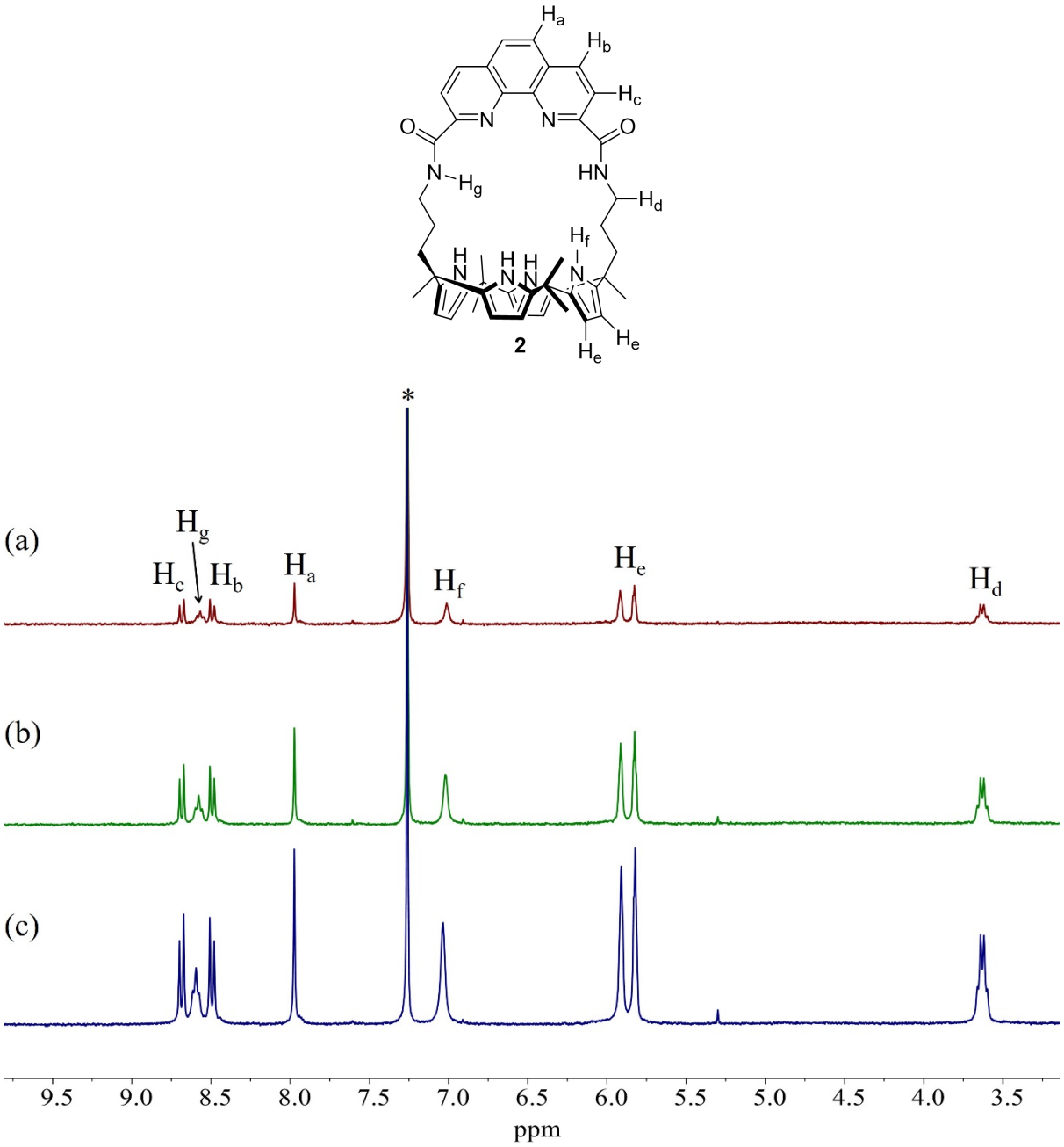

Figure S22. Partial ^{1}H NMR spectra of **2** recorded at different concentrations corresponding to (a) 1.5 mM, (b) 3 mM and (c) 6 mM of receptor **2** in $CDCl_3$.

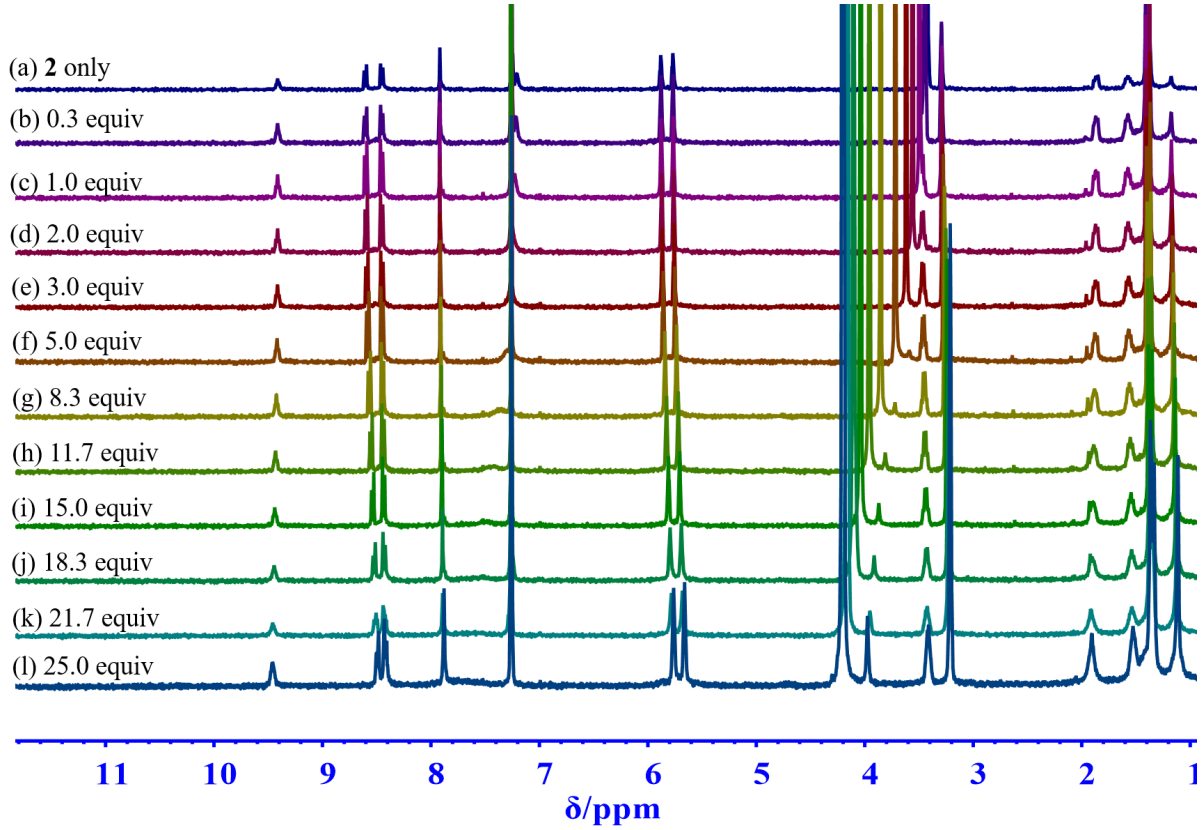

Figure S23. Partial ^{1}H NMR spectra recorded during the titration of **2** (1.4 mM) with LiCl in $CD_3OD/CDCl_3$ (1/9, v/v).

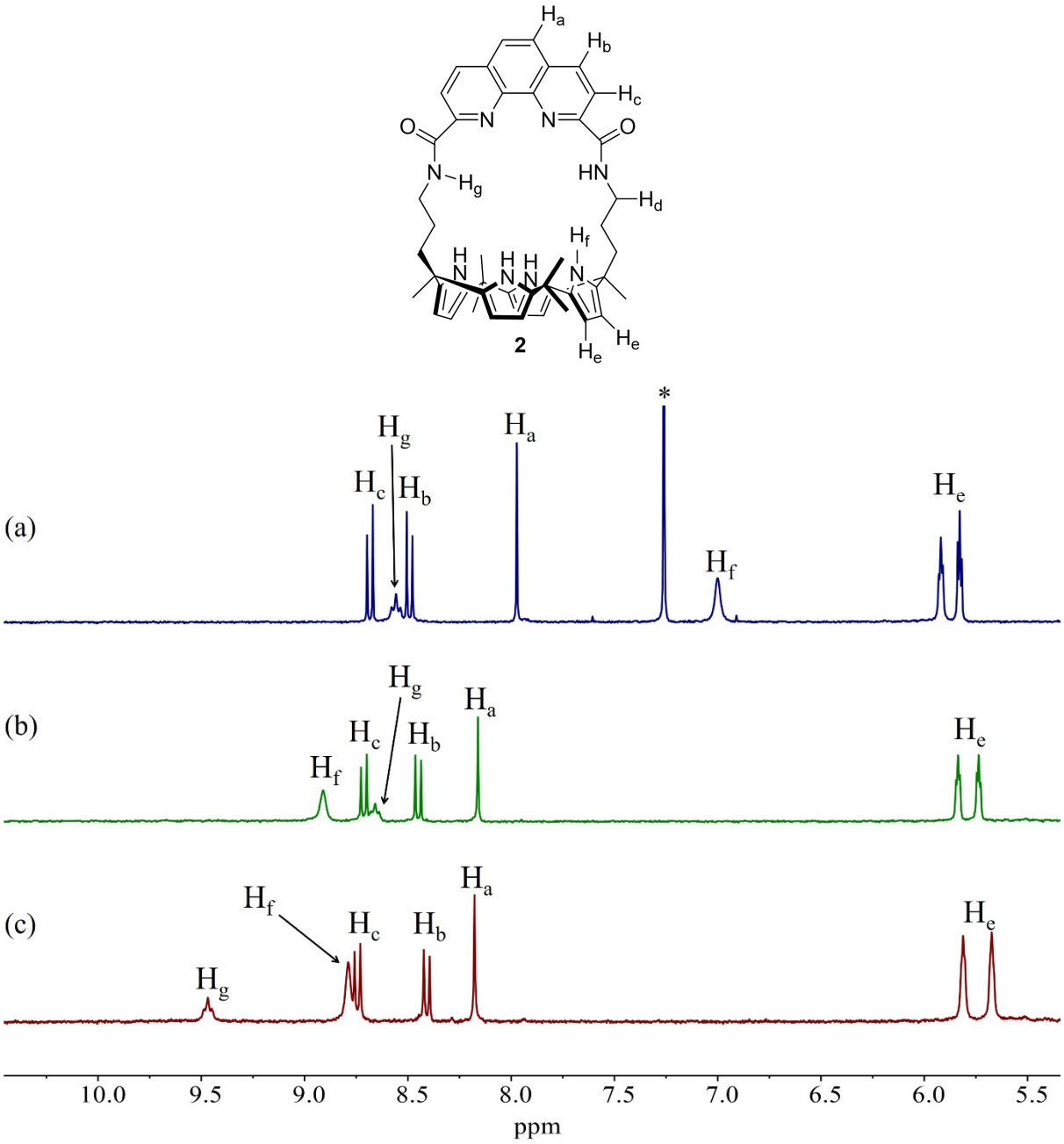

Figure S24. Partial ^{1}H NMR spectra of **2** (3 mM) recorded in (a) $CDCl_3$, (b) DMSO-d_6, and (b) 15% D_2O in DMSO-d_6.

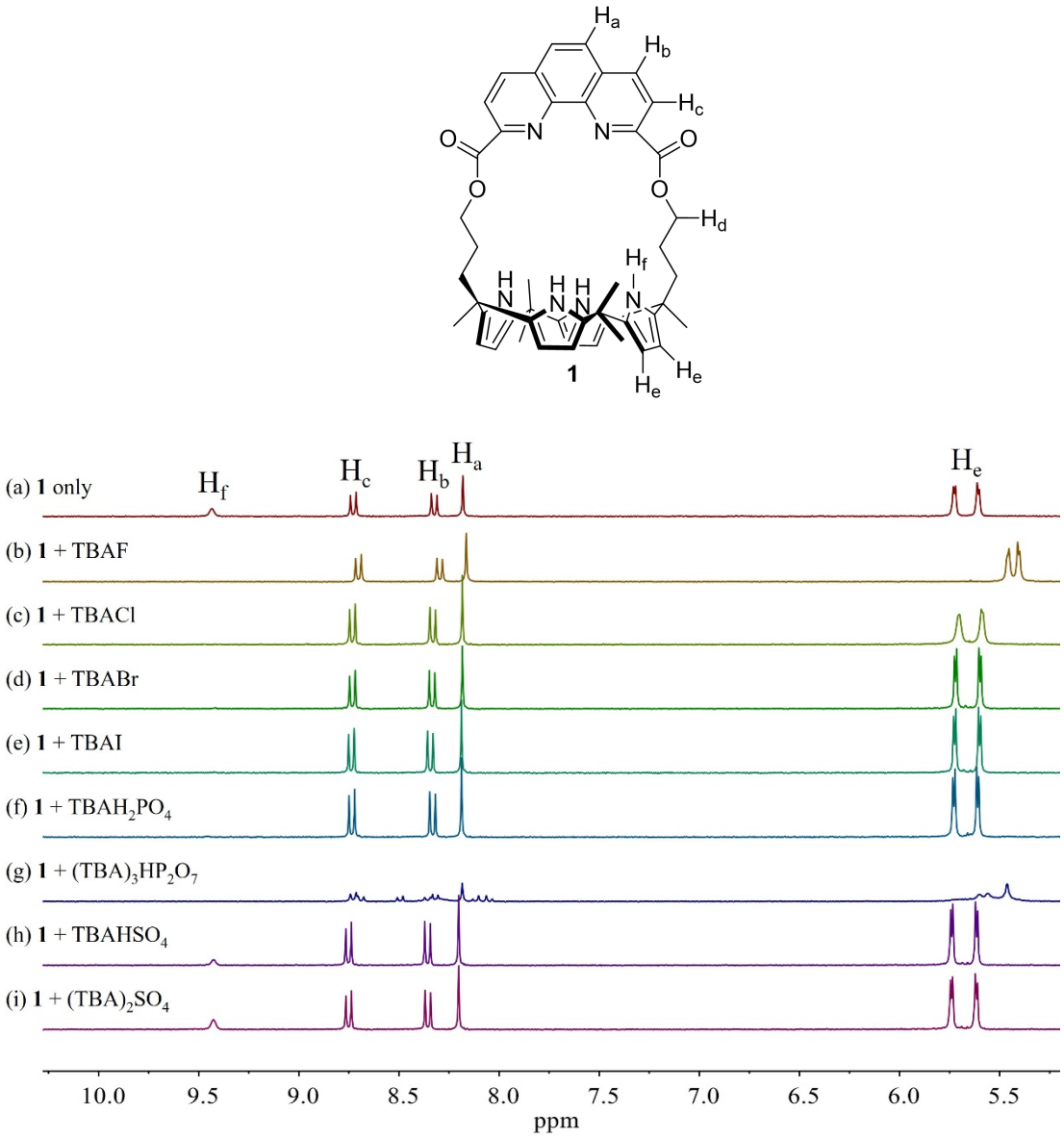

Figure S25. Partial ^{1}H NMR spectra of (a) **1** (3 mM) only, (b) **1** + excess TBAF (tetrabutylammonium fluoride), (c) **1** + excess TBACl, (d) **1** + excess TBABr, (e) **1** + excess TBAI, (f) **1** + excess $TBAH_2PO_4$, (g) **1** + excess $(TBA)_3HP_2O_7$, (h) **1** + excess $TBAHSO_4$, and (i) **1** + excess $(TBA)_2SO_4$ in 15% aqueous DMSO solution (15% D_2O in DMSO-d_6).

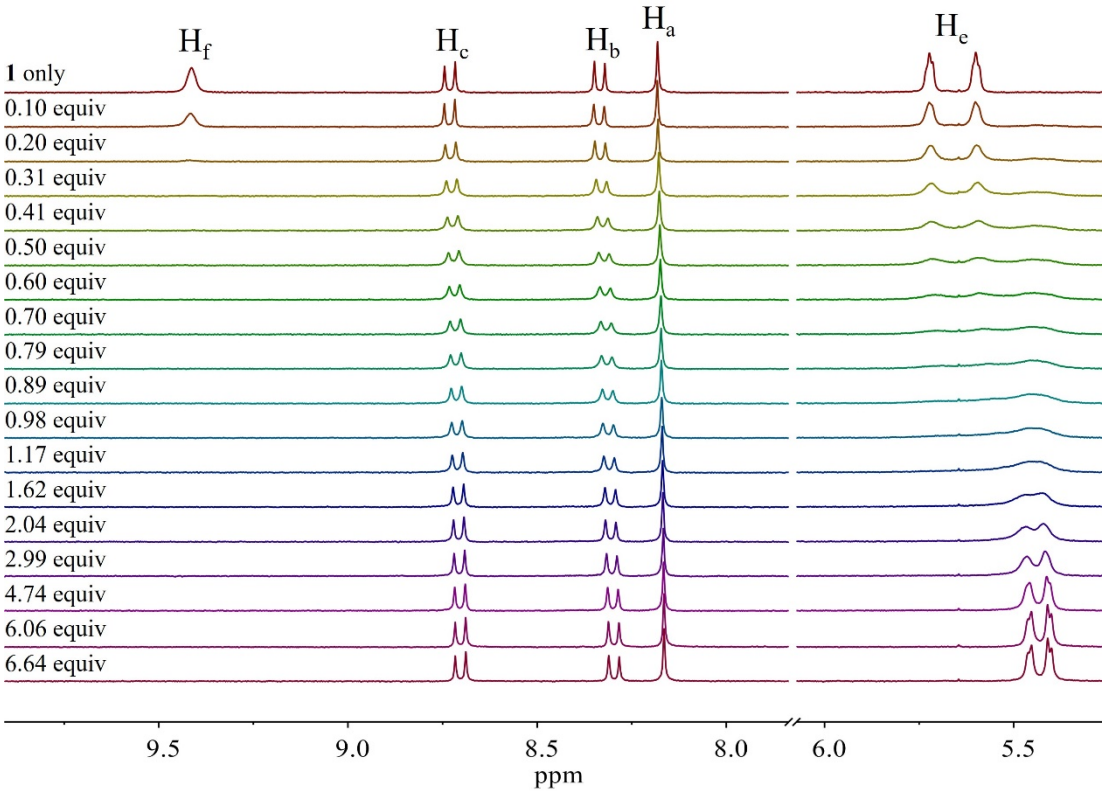

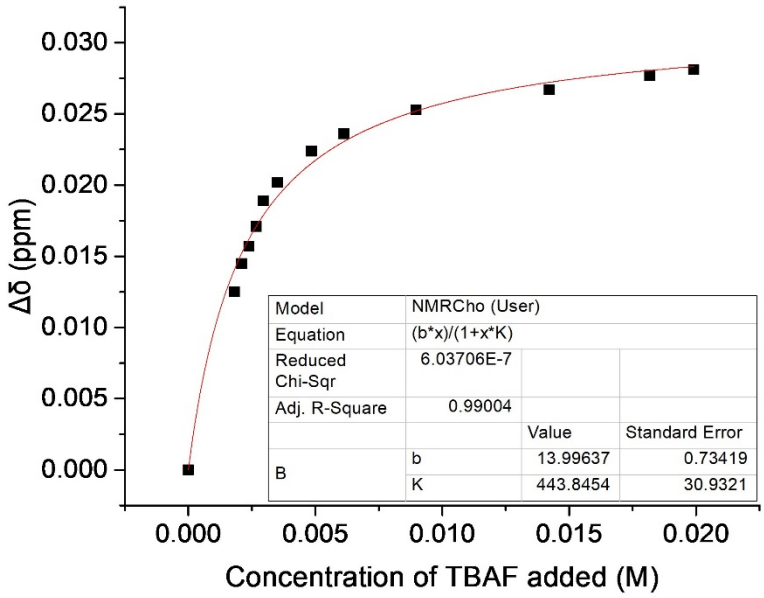

Figure S26. Partial ^{1}H NMR spectra recorded during the titration of **1** (3 mM) with TBAF in aqueous DMSO-d_6 solution (15% D_2O in DMSO-d_6) and the corresponding binding isotherm. The data was fitted based on the chemical shift changes of the signal corresponding to H_c.

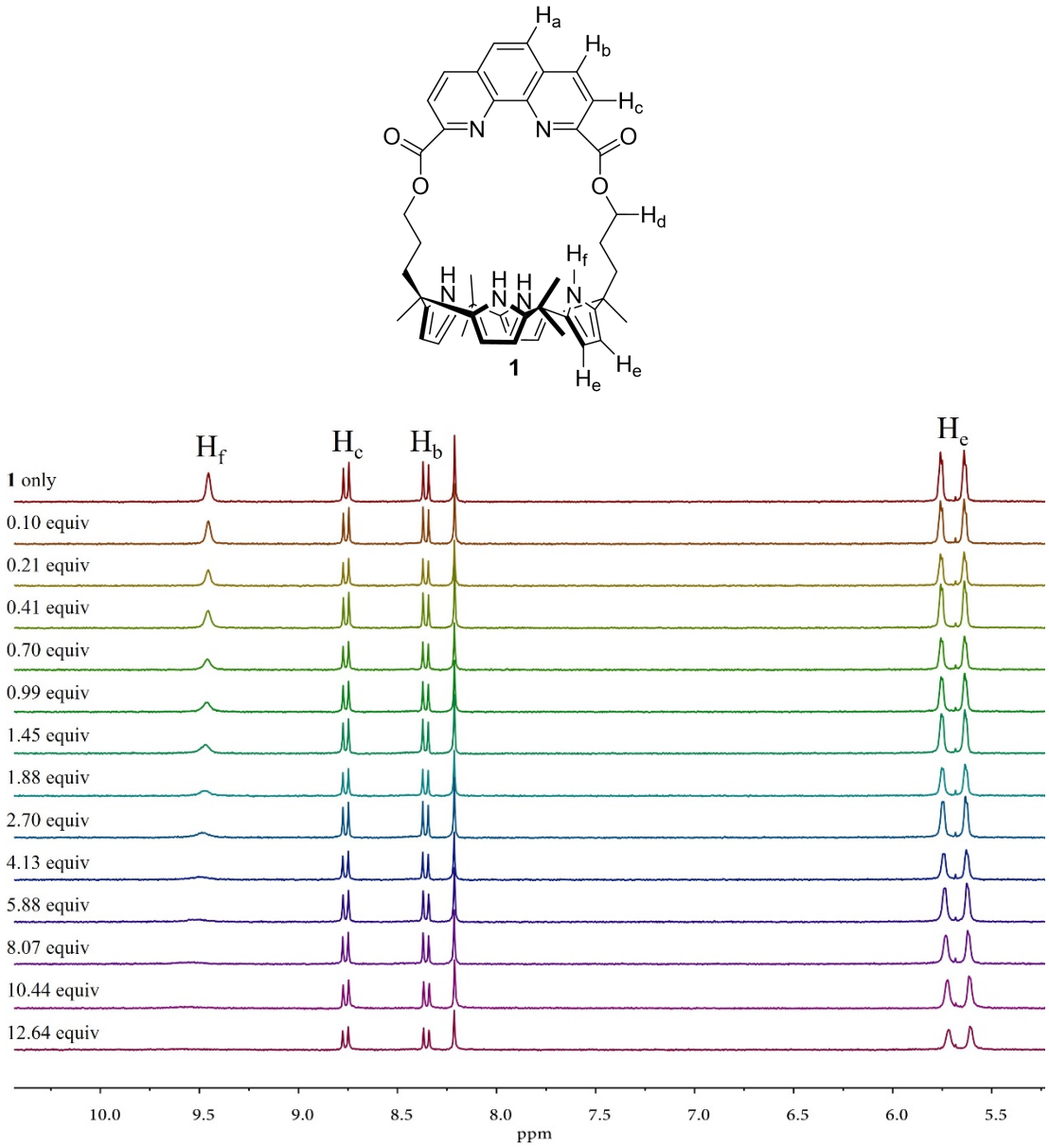

Figure S27. Partial ^{1}H NMR spectra recorded during the titration of **1** (3 mM) with TBACl in 15% aqueous DMSO-d_6 solution (15% D_2O in DMSO-d_6).

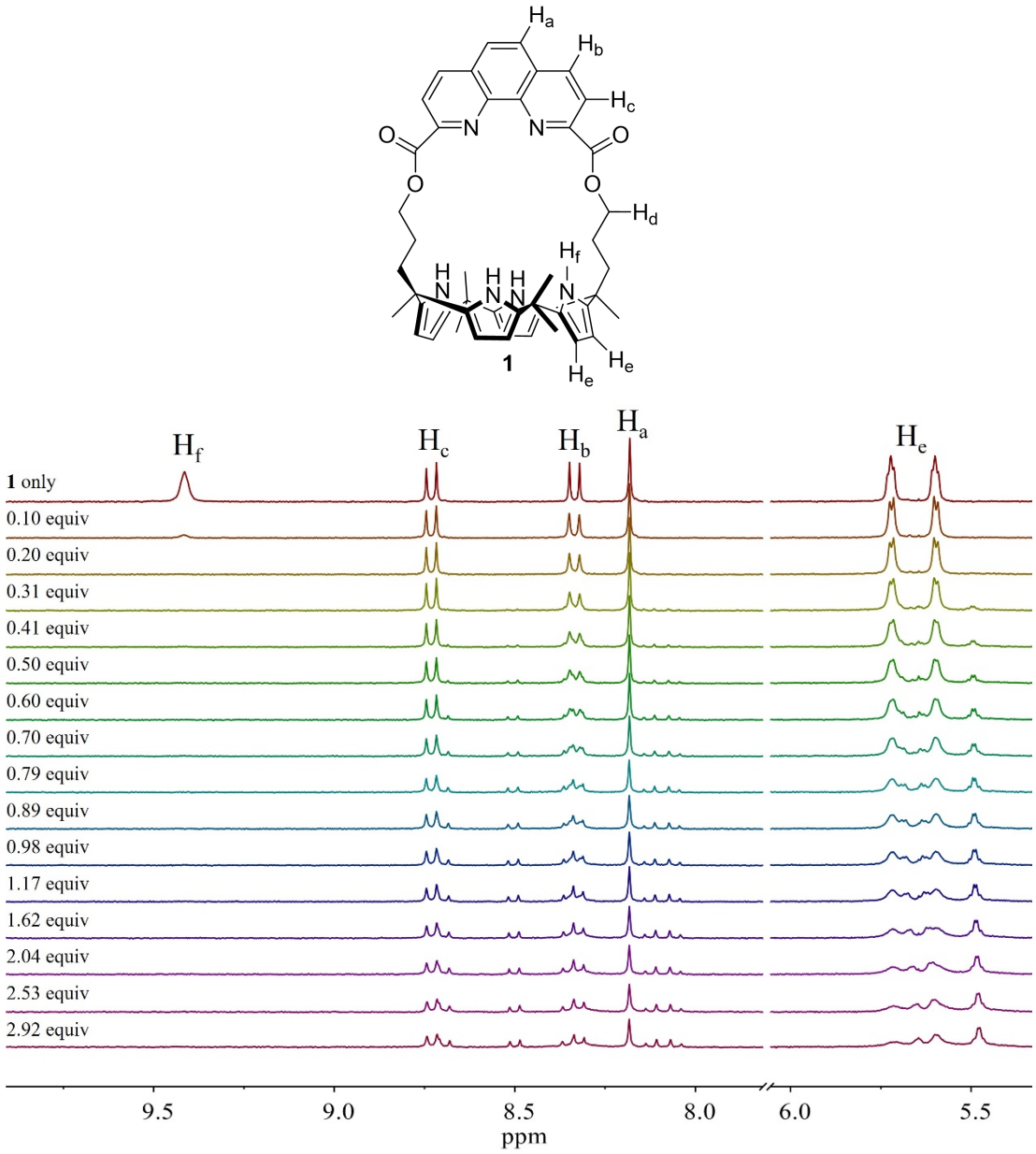

Figure S28. ^{1}H NMR spectra recorded during the titration of **1** (3 mM) with $(TBA)_3HP_2O_7$ in 15% D_2O in DMSO-d_6.

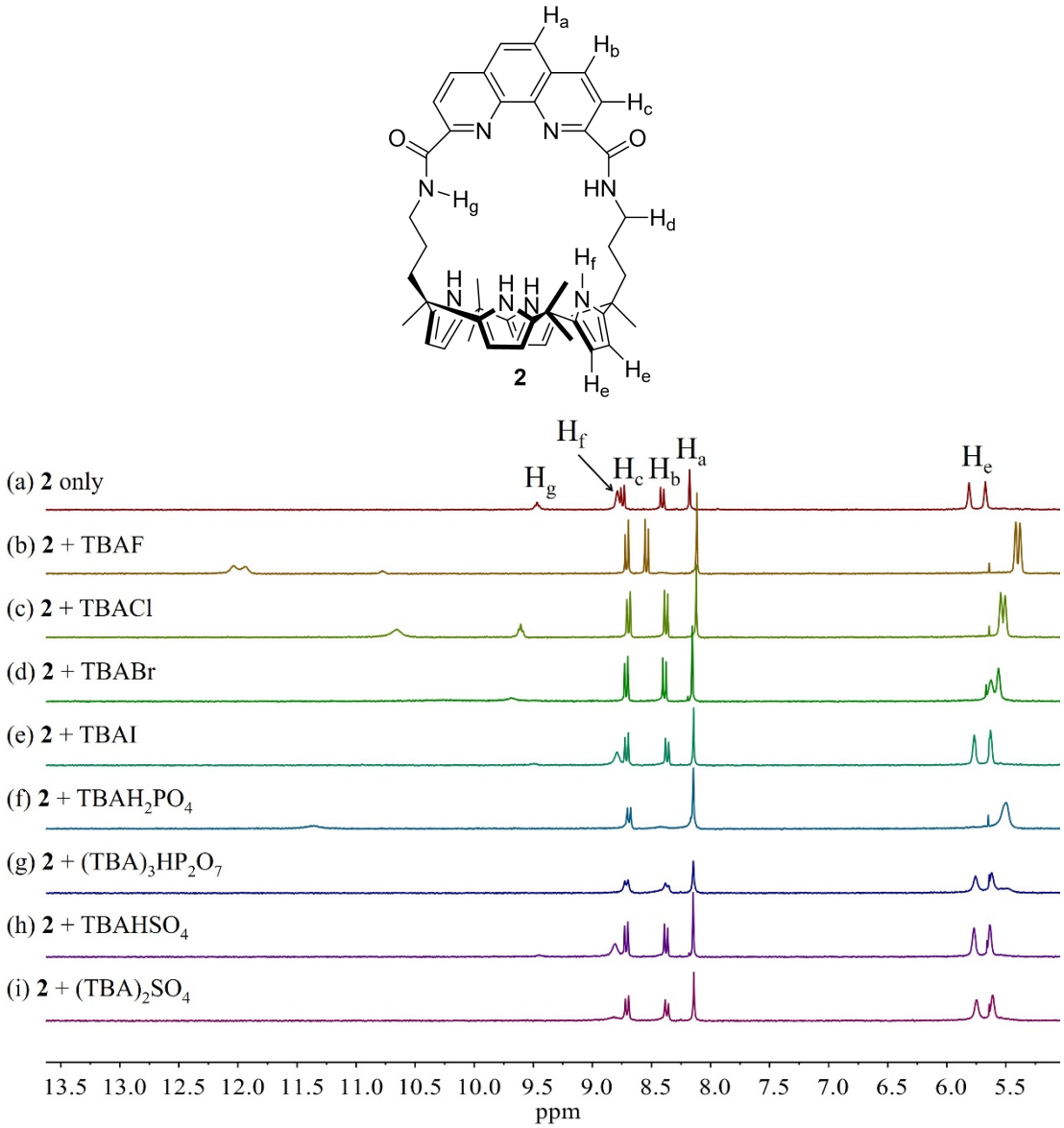

Figure S29. Partial ^{1}H NMR spectra of (a) **2** (3 mM) only, (b) **2** + excess TBAF (tetrabutylammonium fluoride), (c) **2** + excess TBACl, (d) **2** + excess TBABr, (e) **2** + excess TBAI, (f) **2** + excess $TBAH_2PO_4$, (g) **2** + excess $(TBA)_3HP_2O_7$, (h) **2** + excess $TBAHSO_4$, and (i) **2** + excess $(TBA)_2SO_4$ in 15% aqueous DMSO solution (15% D_2O in DMSO-d_6).

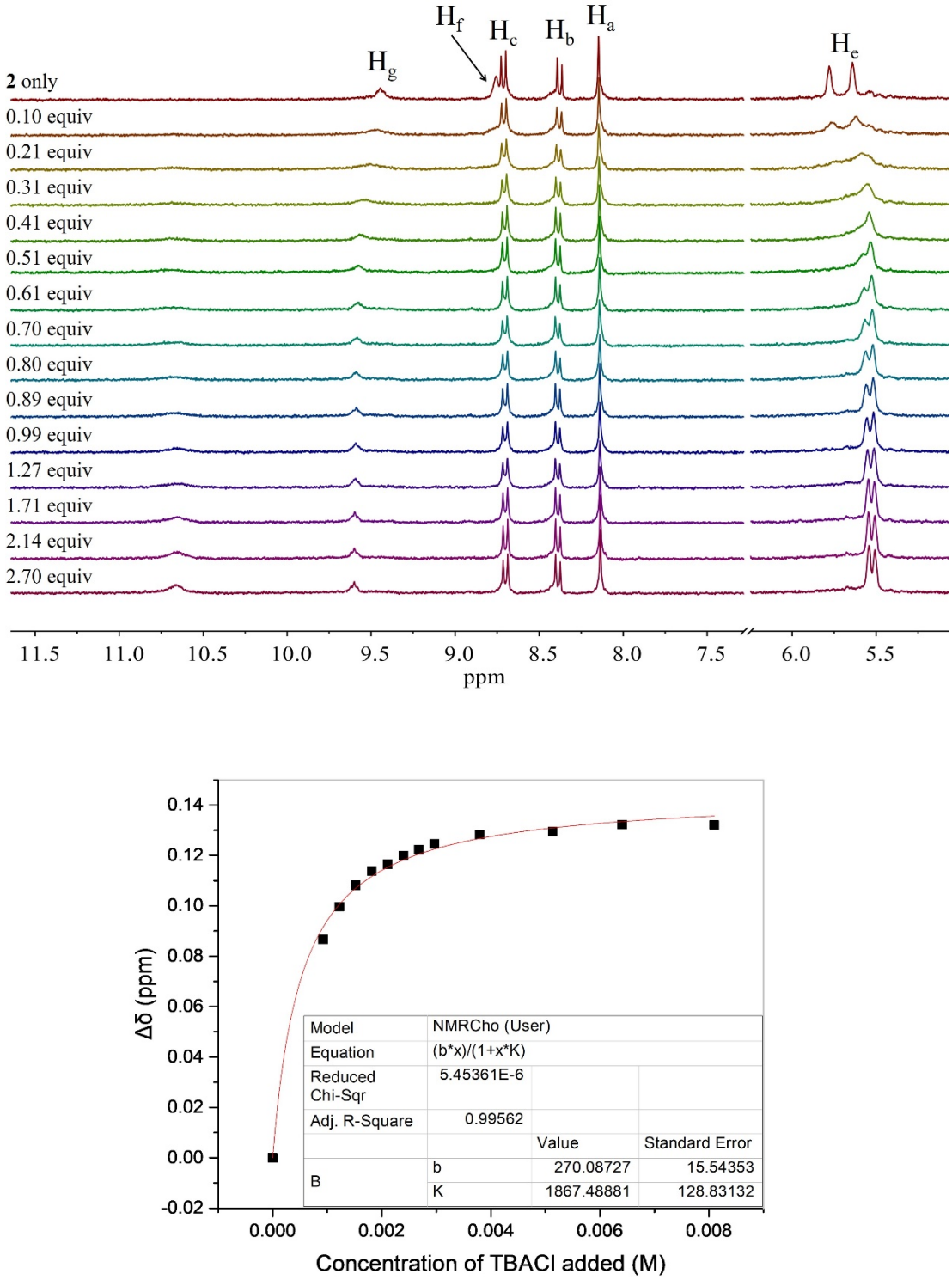

Figure S30. Partial ^{1}H NMR spectra recorded during the titration of **2** (3 mM) with tetrabutylammonium chloride (TBACl) in 15% aqueous DMSO solution (15% D_2O in DMSO-d_6) and the corresponding binding isotherm. The data was fitted based on the chemical shift changes of the signal corresponding to H_e.

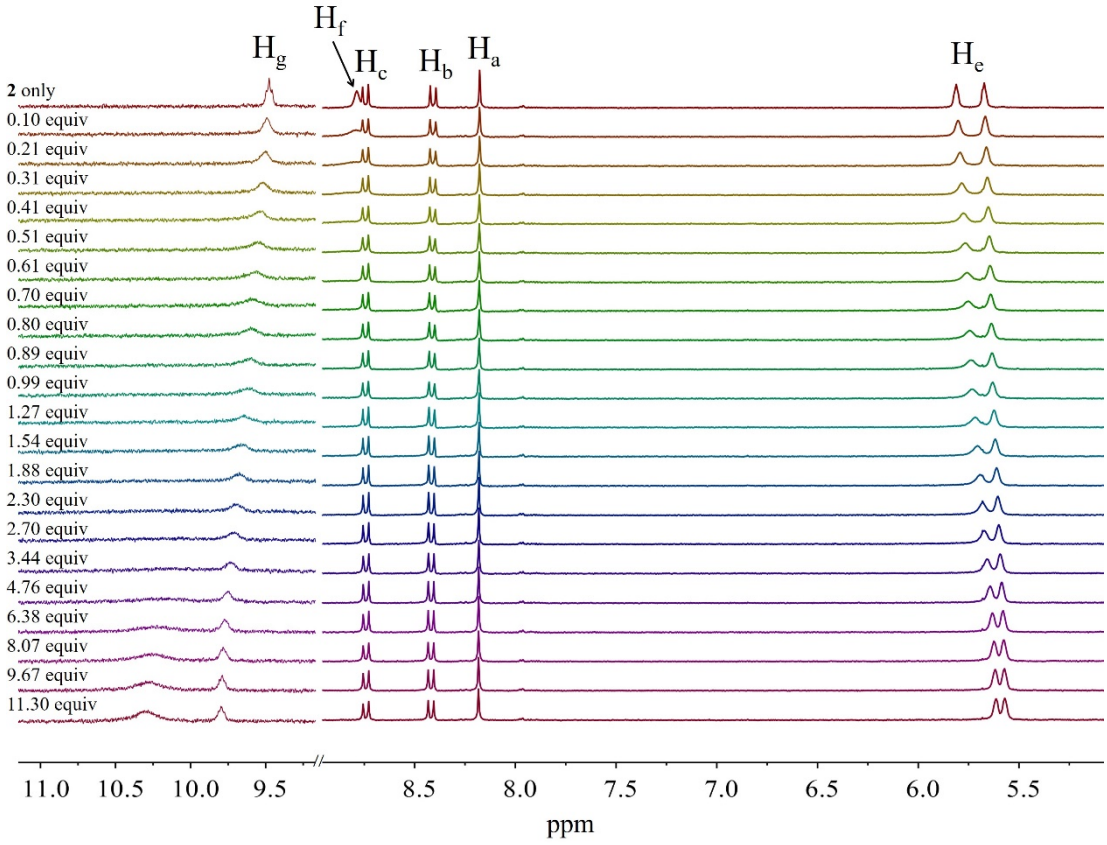

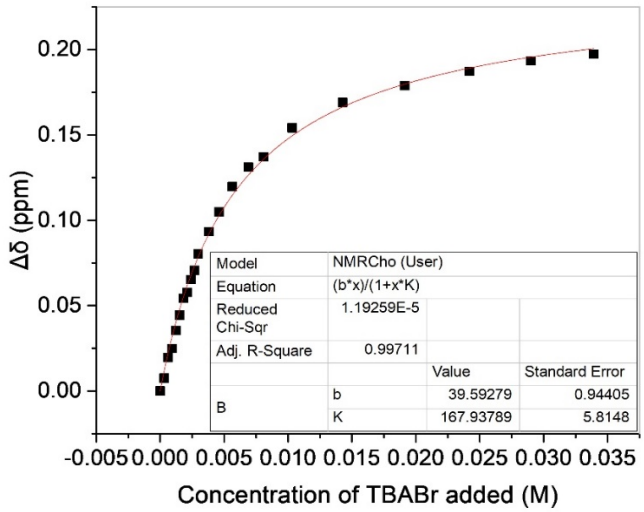

Figure S31. Partial ^{1}H NMR spectra recorded during the titration of **2** (3 mM) with tetrabutylammonium bromide (TBABr) in 15% aqueous DMSO solution (15% D_2O in DMSO-d_6) and the corresponding binding isotherm. The data was fitted based on the chemical shift changes of the signal corresponding to H_e.

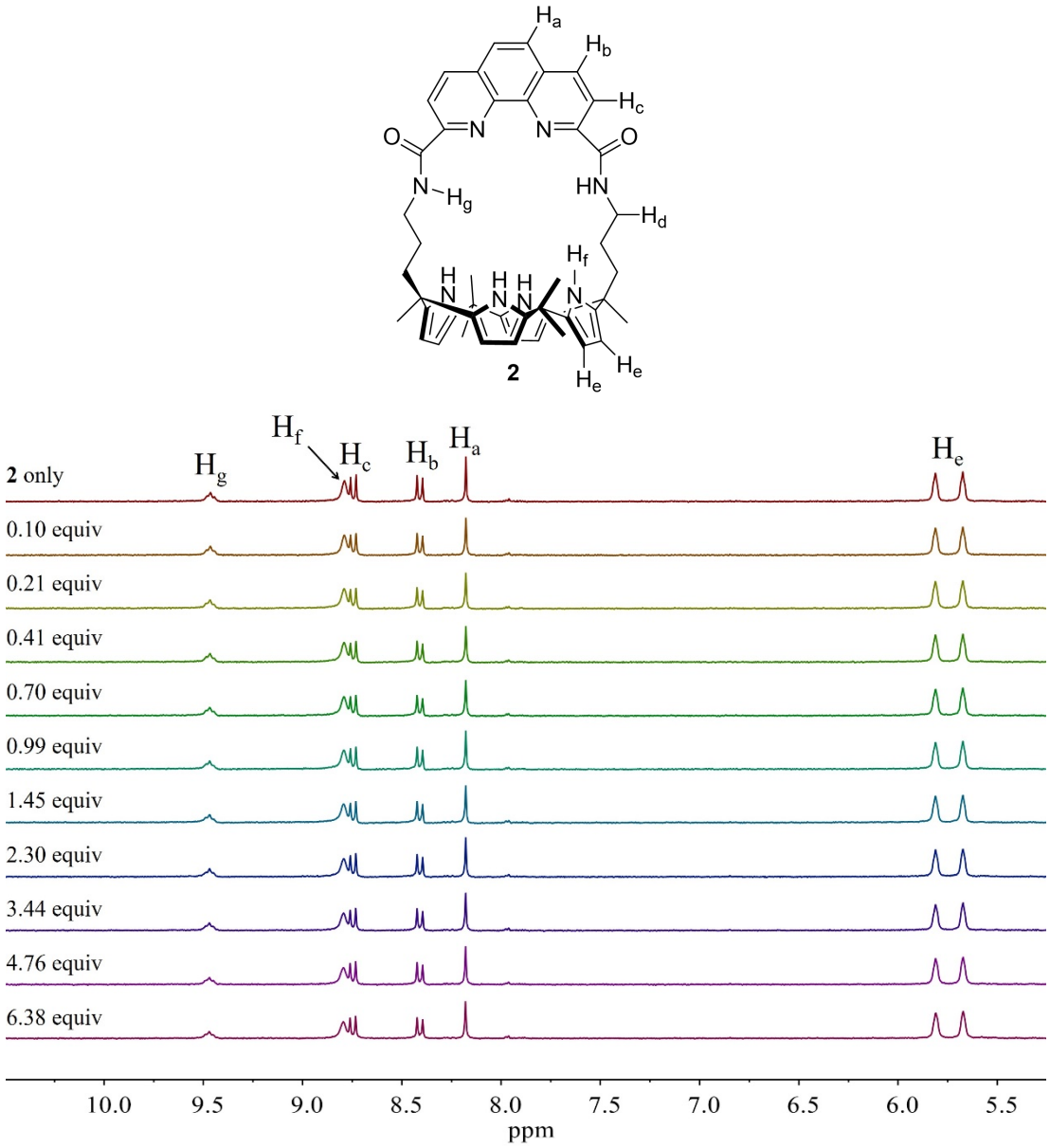

Figure S32. Partial ^{1}H NMR spectra recorded during the titration of **2** (3 mM) with tetrabutylammonium iodide (TBAI) in 15% aqueous DMSO solution (15% D_2O in DMSO-d_6).

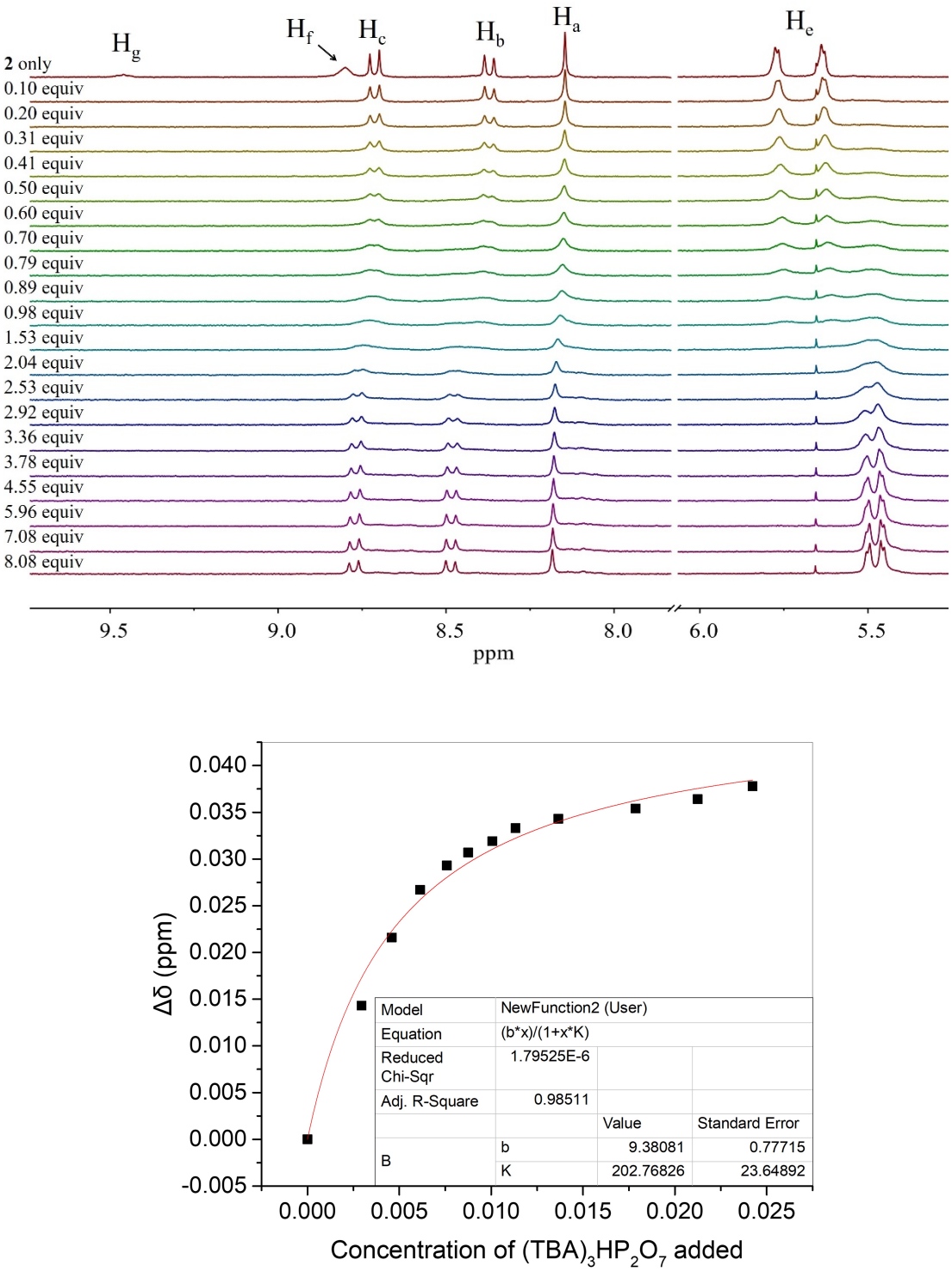

Figure S33. Partial ^{1}H NMR spectra recorded during the titration of **2** (3 mM) with tris(tetrabutylammonium) hydrogen pyrophosphate ($(TBA)_3HP_2O_7$) in 15% aqueous DMSO solution (15% D_2O in DMSO-d_6) and the corresponding binding isotherm. The data was fitted based on the chemical shift changes of the signal corresponding to H_a.

3. NMR spectra and HRMS data

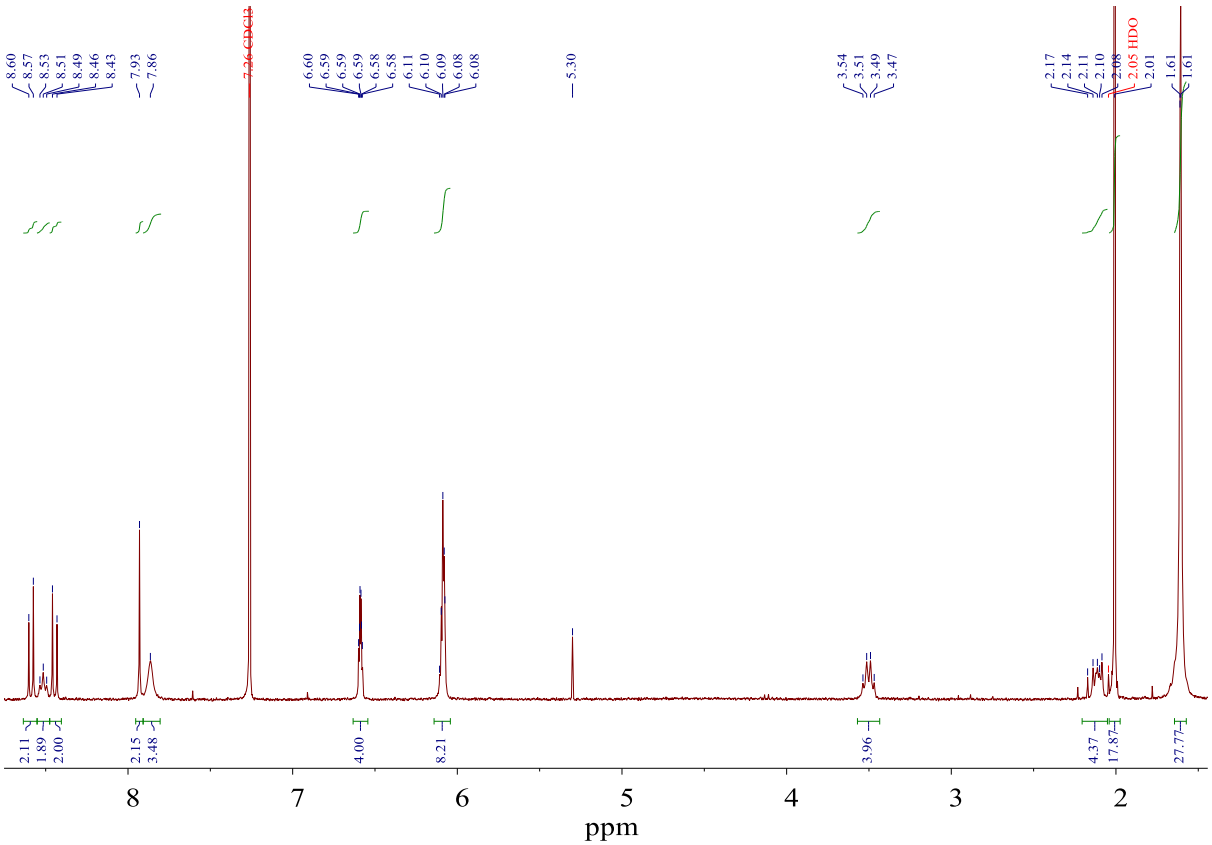

Figure S34. ^{1}H NMR spectrum of **7** recorded in $CDCl_3$.

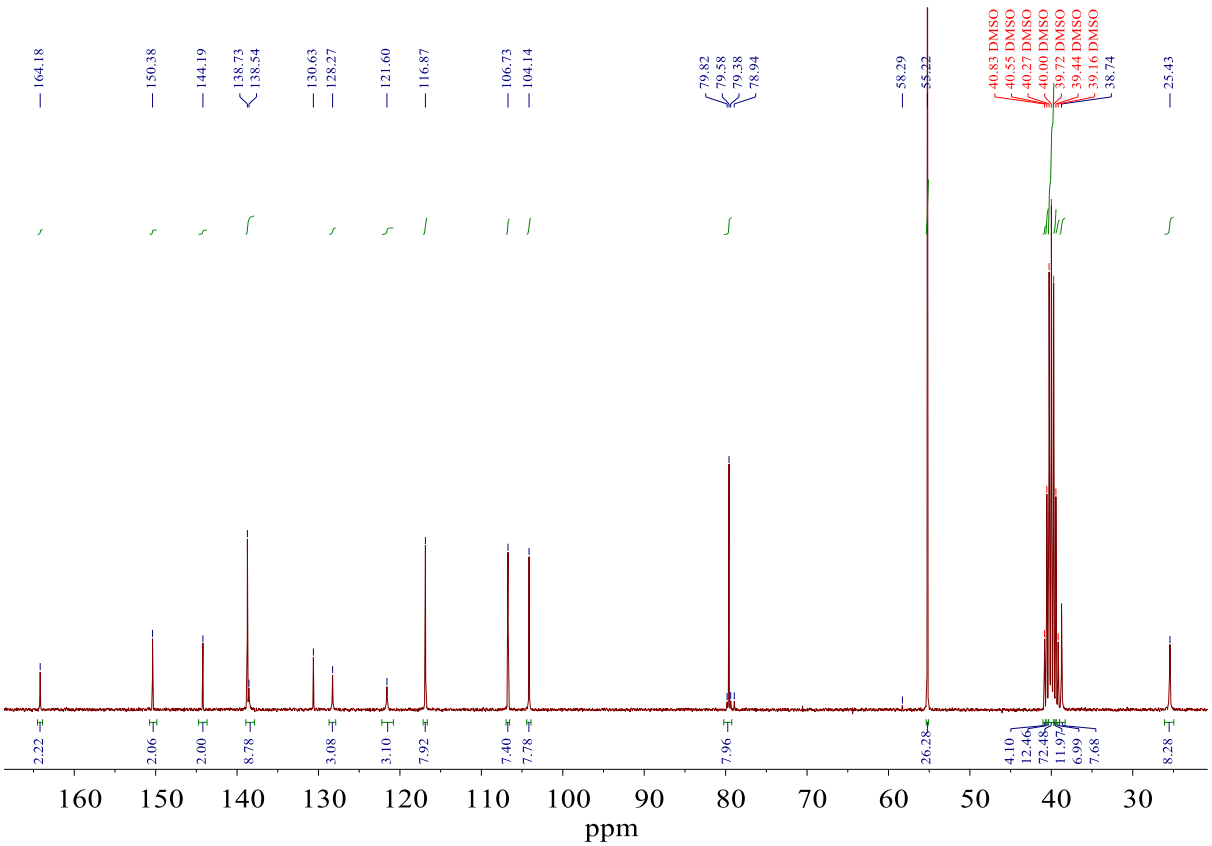

Figure S35. ^{13}C NMR spectrum of **7** recorded in DMSO-d_6.

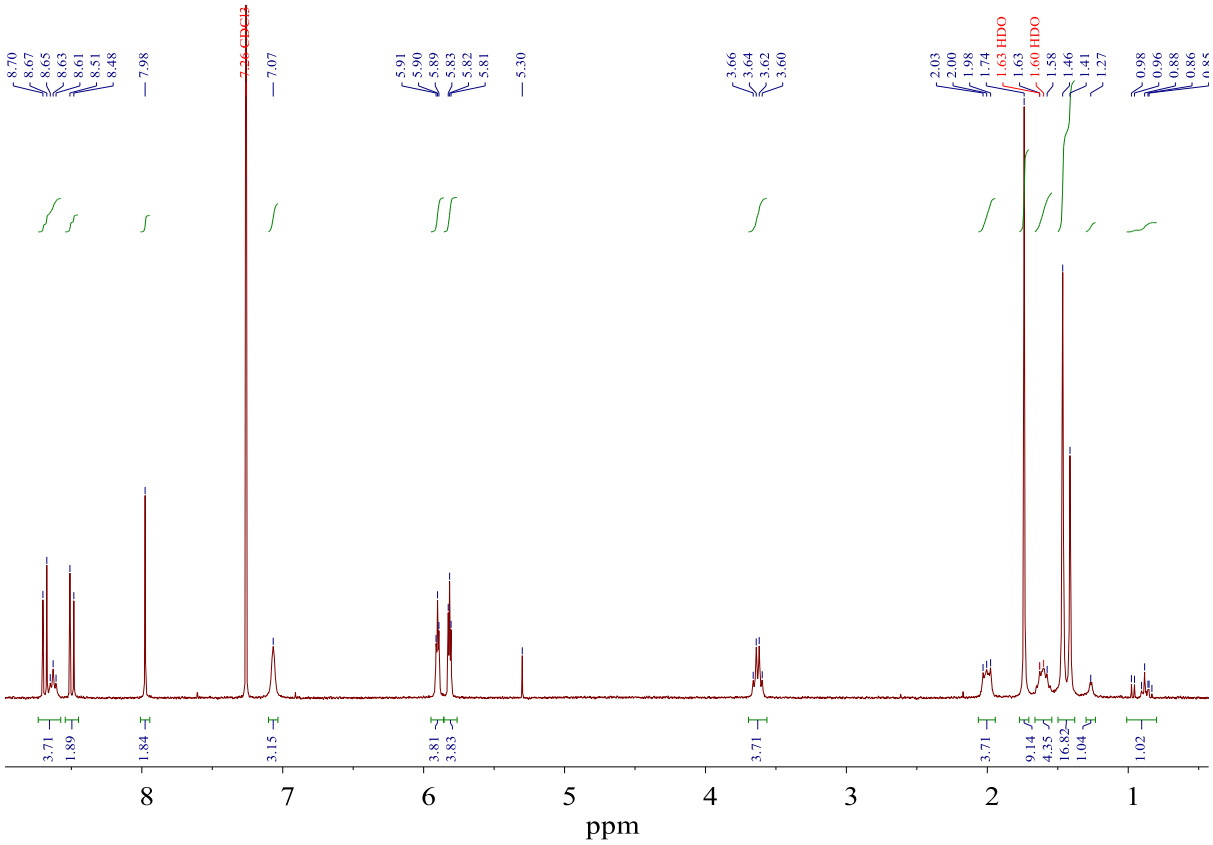

Figure S36. ^{1}H NMR spectrum of **2** recorded in $CDCl_3$.

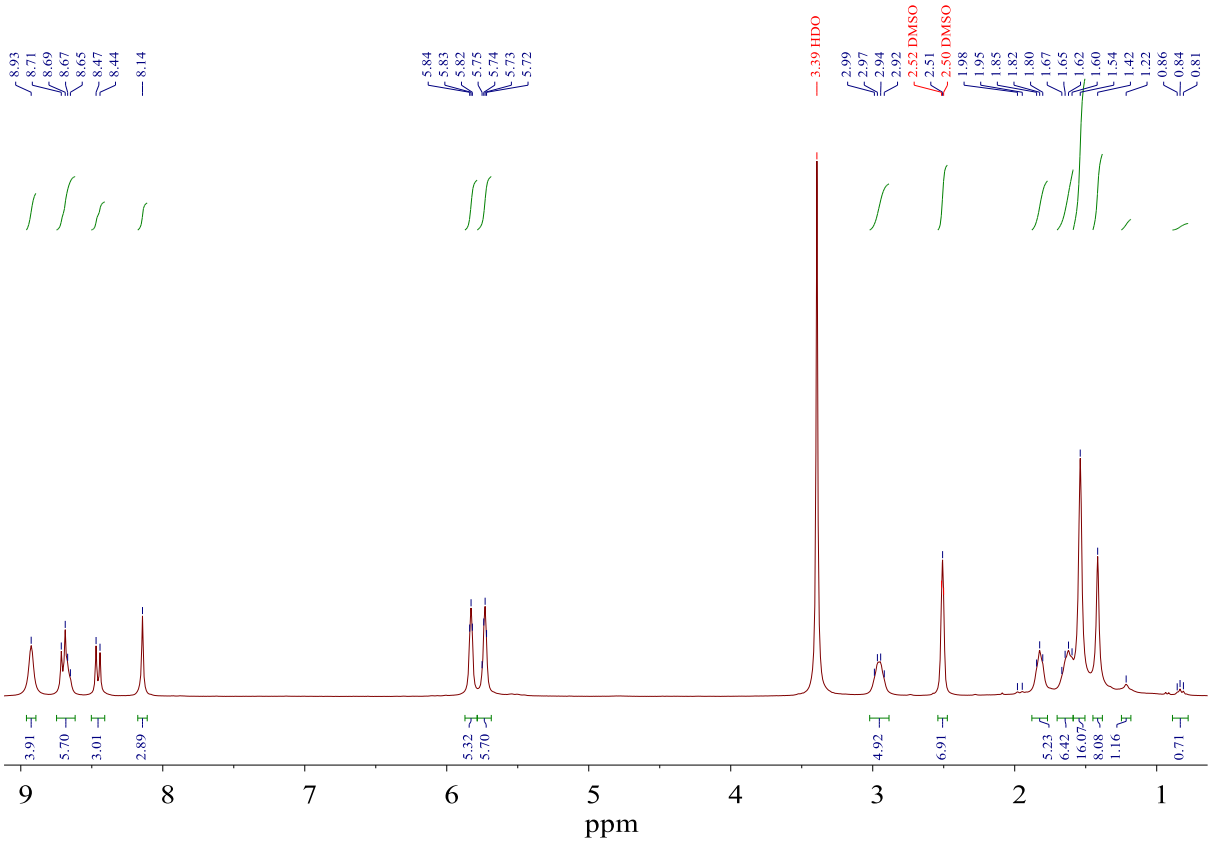

Figure S37. ^{1}H NMR spectrum of **2** recorded in DMSO-d_6.

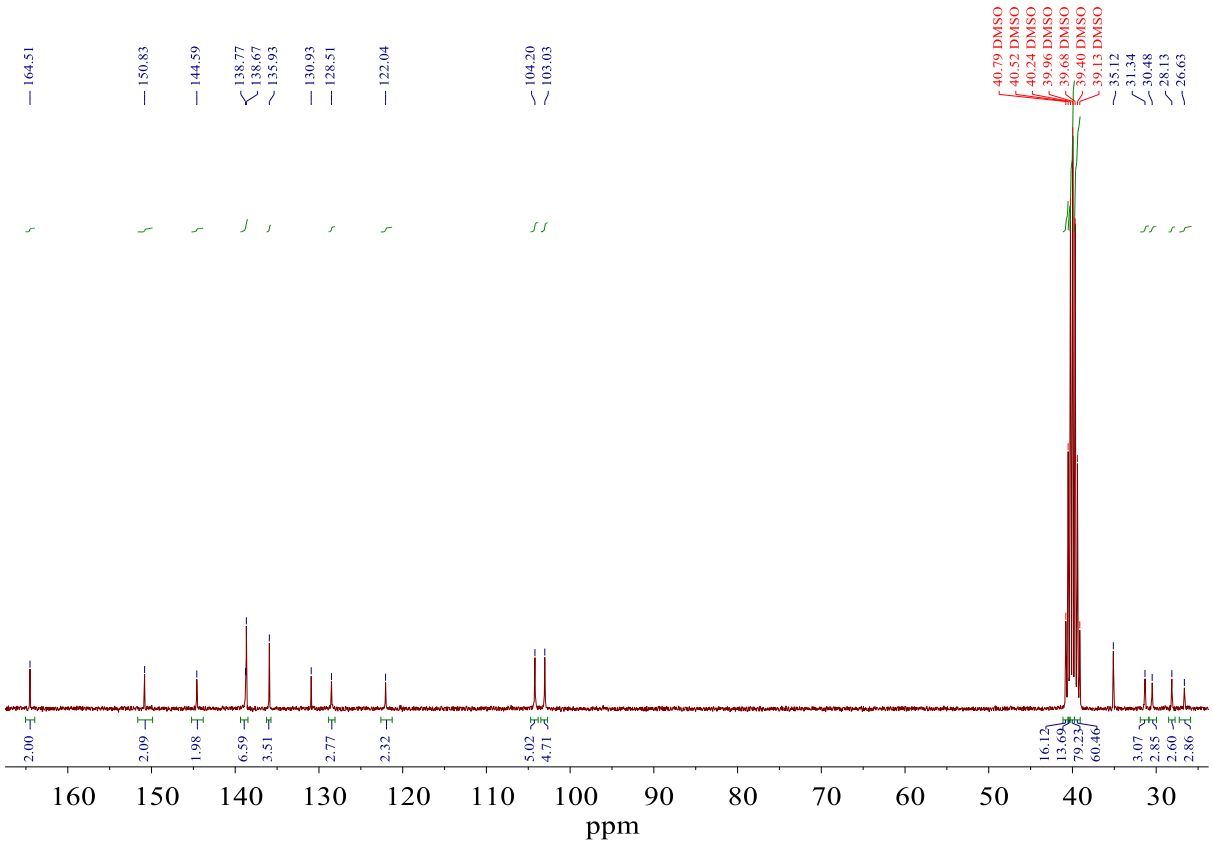

Figure S38. ^{13}C NMR spectrum of **2** recorded in DMSO-d_6.

Target Compound Screening Report

Results Acquired by The University of Texas at Austin Mass Spectrometry Facility

Data File	MSF18-0304(HQ-SKK-amide-trimer)_hrESIpos1.d	**Sample Name**	0304(HQ-SKK-amide-trimer)	**Comment**	0304(HQ-SKK-amide-trimer)
Position	P1-D3	**Instrument Name**	Instrument 1	**User Name**	
Acq Method	pos.m	**Acquired Time**	2/22/2018 11:03:51 AM	**DA Method**	KS.m

MS Zoomed Spectrum

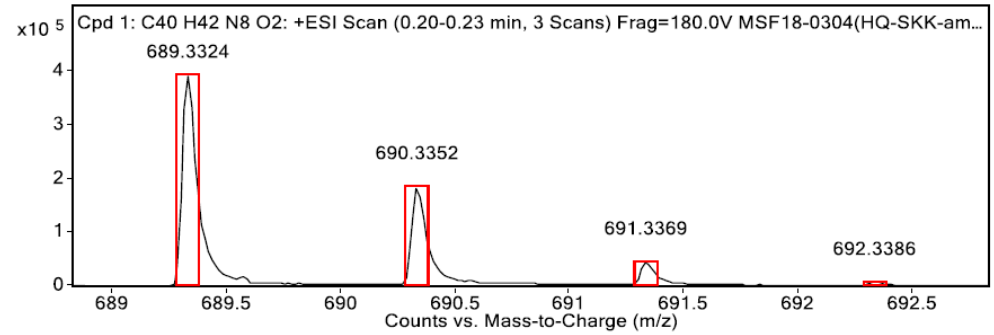

MS Spectrum Peak List

Obs. m/z	Calc. m/z	Charge	Abundance	Formula	Ion Species	Tgt Mass Error (ppm)
689.3324	689.3323	1	391789	C40H42N8O2	(M+Na)+	-0.21
690.3352	690.3353	1	185500	C40H42N8O2	(M+Na)+	0.12
691.3369	691.3382	1	44916	C40H42N8O2	(M+Na)+	1.85
692.3386	692.3411	1	6880	C40H42N8O2	(M+Na)+	3.6
693.3296	693.3439	1	1306	C40H42N8O2	(M+Na)+	20.6

--- End Of Report ---

Figure S39. High resolution ESI mass spectrum of **7**.

Target Compound Screening Report

Results Acquired by The University of Texas at Austin Mass Spectrometry Facility

Data File	MSF18-0305(HQ-SKK-amide-calixpyrrole)_hrESIpos1.d	**Sample Name**	0305(HQ-SKK-amide-calixpyrrole)	**Comment**	0305(HQ-SKK-amide-calixpyrrole)
Position	P1-D4	**Instrument Name**	Instrument 1	**User Name**	
Acq Method	pos.m	**Acquired Time**	2/22/2018 11:08:13 AM	**DA Method**	KS.m

MS Zoomed Spectrum

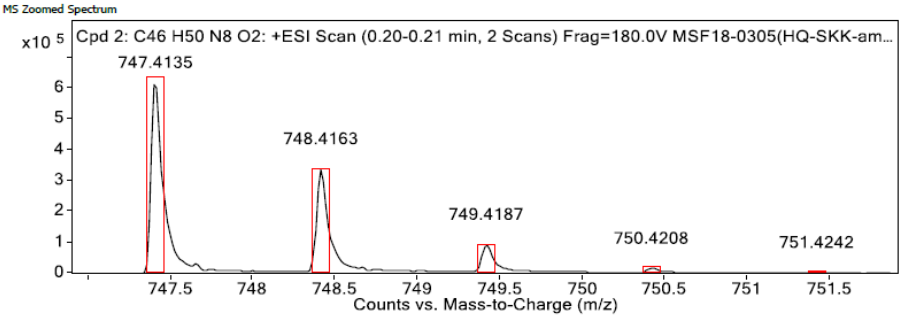

MS Spectrum Peak List

Obs. m/z	Calc. m/z	Charge	Abundance	Formula	Ion Species	Tgt Mass Error (ppm)
747.4135	747.4129	1	632264	C46H50N8O2	(M+H)+	-0.68
748.4163	748.4160	1	338809	C46H50N8O2	(M+H)+	-0.36
749.4187	749.4190	1	93529	C46H50N8O2	(M+H)+	0.43
750.4208	750.4219	1	15784	C46H50N8O2	(M+H)+	1.48
751.4242	751.4248	1	2244	C46H50N8O2	(M+H)+	0.78

--- End Of Report ---

Figure S40. High resolution ESI mass spectrum of **2**.

4. X-ray experimental for the complex 2·TBACl

Single crystals of **2**·TBACl complex were obtained as colorless prisms via the slow evaporation of a $CHCl_3/CH_3OH$ solution of receptor **2** in the presence of excess TBACl. A suitable crystal was selected and the data were collected on a Rigaku AFC12 diffractometer with a Saturn 724+ CCD with MoKα irradiation (λ = 0.71075 Å). The crystal was kept at 100.15 K during data collection. Using Olex2,[3] the structure was solved with the ShelXT[4] structure solution program using Direct Methods and refined with the ShelXL[5] refinement package using Least Squares minimization. Tables of positional and thermal parameters, bond lengths and angles, torsion angles and figures are in the CIF. CCDC deposition number: 1965677.

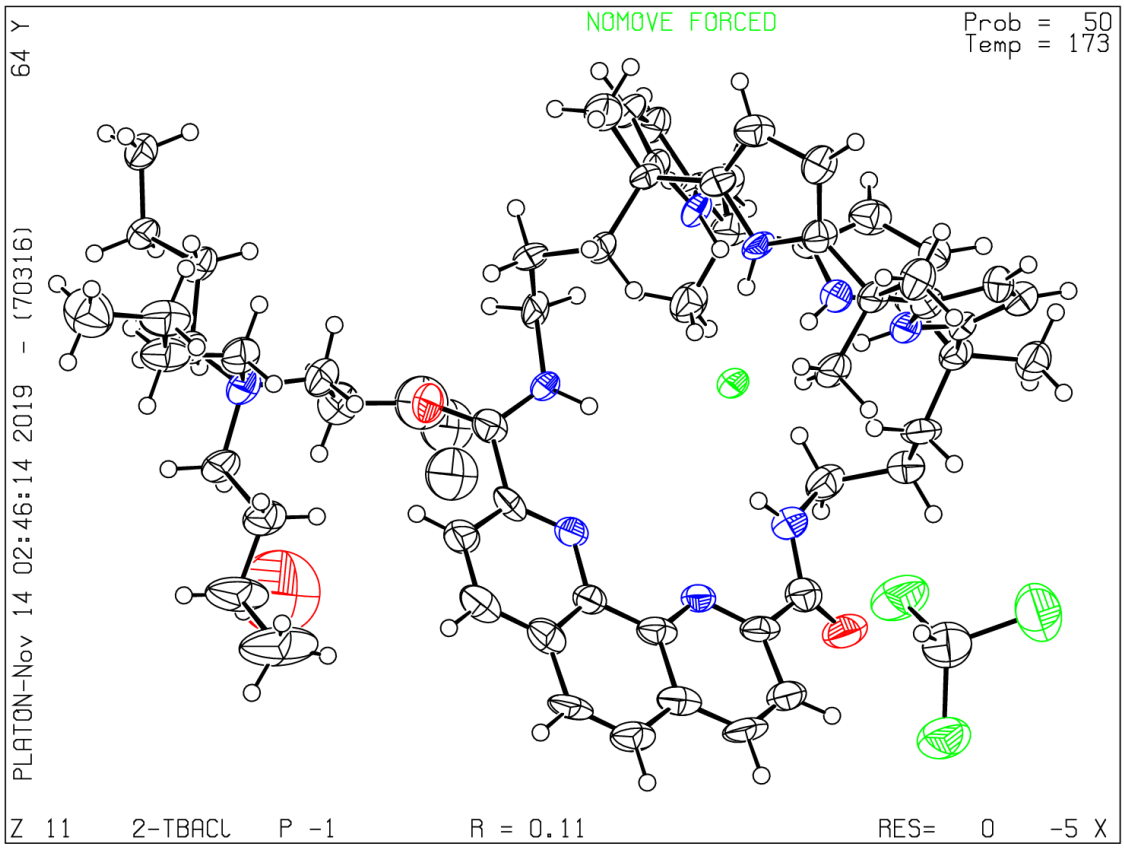

Figure S41. View of **2**·TBACl complex. Displacement ellipsoids are scaled to the 50% probability level.

Table 1 Crystal data and structure refinement for 2-TBACl.

Identification code	2-TBACl
Empirical formula	$C_{63}H_{82}Cl_4N_9O_3$
Formula weight	1155.17
Temperature/K	173.15
Crystal system	triclinic
Space group	P-1
a/Å	13.0780(8)
b/Å	14.7017(11)
c/Å	16.4585(12)
α/°	89.009(6)
β/°	84.136(6)
γ/°	81.419(6)
Volume/Å^3	3112.7(4)
Z	2
ρ_{calc}g/cm^3	1.233
μ/mm^{-1}	0.242
F(000)	1230.0
Crystal size/mm^3	0.080 × 0.078 × 0.059
Radiation	MoKα (λ = 0.71075 Å)
2Θ range for data collection/°	3.166 to 45.542
Index ranges	$-14 \leq h \leq 14$, $-15 \leq k \leq 15$, $-17 \leq l \leq 17$
Reflections collected	26770
Independent reflections	8306 [R_{int} = 0.1213, R_{sigma} = 0.1537]
Data/restraints/parameters	8306/456/711
Goodness-of-fit on F^2	1.036
Final R indexes [I>=2σ (I)]	R_1 = 0.1052, wR_2 = 0.2447
Final R indexes [all data]	R_1 = 0.2048, wR_2 = 0.3060
Largest diff. peak/hole / e Å^{-3}	0.46/-0.47
CCDC number	1965677

5. Energies and geometrical coordinates of the optimized structures in the gas phase

All calculations were carried out with the Gaussian 09 suite[6] of programs using the X3LYP density functional.[7] Complexation energies were corrected for basis set superposition error (BSSE) using the counterpoise correction method.[8, 9]

1·HCO_3^- complex

Number of negative frequencies: 0

Counterpoise corrected energy = -2674.641528069306

BSSE energy = 0.007267290393

sum of fragments = -2674.551805908503

complexation energy = -60.86 kcal/mole (raw)

complexation energy = -56.30 kcal/mole (corrected)

Cartesian coordinates:

Symbol	X	Y	Z
O	-1.92576300	2.88093900	-1.85268600
O	-2.76392000	4.68294900	-0.78148000
O	-2.66890500	-4.76611700	-1.72977600
O	-1.48391100	-2.94255800	-1.10119200
N	3.22955500	0.84108800	-1.70270800
H	2.27172200	0.51659700	-1.55555800
N	1.81475400	2.23263600	1.09794800
H	1.54504000	1.34206500	0.67494700
N	1.22484600	-0.74037100	2.53808900
H	0.45891200	-0.59839100	1.86753700
N	2.83862400	-2.12449800	-0.24801000
H	2.16904600	-1.34945600	-0.27306300
N	-3.86221400	1.28685900	-0.68429400
N	-3.81543500	-1.51354000	-0.85257400
C	4.29268900	0.02975600	-2.02103500
C	5.42352100	0.82775100	-2.00157700
H	6.43254700	0.50620900	-2.22170100
C	5.01757100	2.14649100	-1.65380800
H	5.66335700	3.00892000	-1.55961200
C	3.64569100	2.12983800	-1.46695400
C	2.65997500	3.23733700	-1.10136100
C	2.38858100	3.27831100	0.39901100
C	2.65055000	4.27884500	1.31649500
H	3.10450800	5.23595100	1.09969200
C	2.23208100	3.81863100	2.59361200
H	2.30052300	4.36681600	3.52274500
C	1.71682500	2.54427300	2.43988200
C	1.07518800	1.62993000	3.48141300
C	1.64494300	0.21778100	3.43717200
C	2.63723500	-0.35955500	4.21038600

H	3.18281500	0.12536200	5.00817800
C	2.81485300	-1.69305400	3.76245800
H	3.53204000	-2.40675300	4.14507700
C	1.92990600	-1.91387700	2.72131300
C	1.79592600	-3.14962200	1.83213200
C	2.83497100	-3.10678200	0.71805100
C	3.89707800	-3.94926600	0.44169500
H	4.18006600	-4.82378600	1.01112400
C	4.55431200	-3.45128100	-0.71770700
H	5.42193300	-3.88397100	-1.19612100
C	3.88171400	-2.31595000	-1.13162000
C	4.09791500	-1.44104100	-2.36221400
C	3.28531000	4.58166600	-1.52611500
H	2.63675300	5.42232400	-1.26413400
H	3.45598300	4.59071800	-2.60777700
H	4.24618100	4.73944300	-1.02851900
C	1.35179800	2.21810800	4.88090000
H	0.92390900	1.56635700	5.64900100
H	0.89475900	3.20872200	4.97467000
H	2.42425400	2.32090500	5.07122900
C	-0.46345900	1.61494400	3.28222000
H	-0.75383900	1.22357100	2.30462000
H	-0.85011500	2.63697700	3.37301900
H	-0.93866200	0.99242800	4.05105700
C	2.05740700	-4.40270700	2.69564300
H	1.93232400	-5.31696900	2.10476800
H	1.35389400	-4.42833900	3.53349600
H	3.07221300	-4.40678700	3.10293800
C	2.87714200	-1.59344200	-3.31048900
H	1.94824400	-1.26073000	-2.83755400
H	2.75424300	-2.64589700	-3.59209600
H	3.02357500	-1.00021200	-4.22101700
C	5.34662700	-1.94037100	-3.11257500
H	5.51715200	-1.32814800	-4.00361400
H	5.21415100	-2.98150900	-3.42455000
H	6.23909900	-1.88529800	-2.48156200
C	1.33798700	3.00353900	-1.90266000
H	1.60899200	2.89776900	-2.96287700
H	0.89476000	2.05053300	-1.60342600
C	0.26682600	4.09151400	-1.77731900
H	0.01345200	4.28168200	-0.72921000
H	0.63991800	5.04247900	-2.17943300
C	-1.00585700	3.75878400	-2.55940700
H	-1.55422300	4.66976200	-2.81080600
H	-0.77535000	3.20375300	-3.47183700
C	-2.77706700	3.49020600	-1.03437600
C	-3.86776700	2.59885000	-0.48392600
C	-4.90304500	3.28385900	0.19127100
H	-4.81024000	4.35252600	0.33573300
C	-5.99975700	2.56994000	0.60430800
H	-6.83562900	3.05915300	1.09846800
C	-6.04894300	1.18093000	0.37323500
C	-4.91930000	0.56702600	-0.24548200
C	-4.92877800	-0.88644100	-0.41508900

C	-6.11479700	-1.60198600	-0.07132900
C	-6.12915700	-2.99500600	-0.28436600
H	-7.02925800	-3.56061300	-0.05577800
C	-4.99829700	-3.61776000	-0.75205400
H	-4.94435300	-4.68570200	-0.92286500
C	-3.84662500	-2.83372300	-0.98406000
C	-2.59981000	-3.61317600	-1.33692800
C	-0.22519100	-3.66570000	-1.21519600
H	0.49111400	-2.90068200	-1.51339700
H	-0.32616100	-4.41583200	-2.00211700
C	0.15598200	-4.29611800	0.12261400
H	1.08356300	-4.85636500	-0.04941500
H	-0.61211400	-5.03345300	0.38515000
C	0.34642300	-3.25980600	1.25742100
H	-0.31710700	-3.49789800	2.09792800
H	0.00453200	-2.28908600	0.89919500
C	-7.20104300	0.41040500	0.73126800
H	-8.04427400	0.92387200	1.18630100
C	-7.24259600	-0.92598500	0.49417400
H	-8.12211200	-1.51181500	0.74933800
C	-0.37497100	-0.10319100	-0.43849900
O	-0.95653000	-0.24853300	0.65834100
O	-1.10531300	0.02792000	-1.57173600
O	0.89054300	-0.06453200	-0.60861200
H	-2.04606600	-0.01022500	-1.30336400

2·HCO_3^- complex

Number of negative frequencies: 0

Counterpoise corrected energy = -2634.946344239856

BSSE energy = 0.007224049726

sum of fragments = -2634.829374015003

complexation energy = -77.93 kcal/mole (raw)

complexation energy = -73.40 kcal/mole (corrected)

Cartesian coordinates:

Symbol	X	Y	Z
O	-3.45666900	4.61181100	-2.04407000
O	-2.78369800	-4.84106400	-1.03151500
N	3.39580000	1.21429400	-1.34190700
H	2.47745200	0.82023800	-1.14552100
N	1.86436500	1.99376500	1.61266900
H	1.39144300	1.36693300	0.96026800

N	1.43974800	-1.23060400	2.20854500
H	1.10551600	-0.77347300	1.36295400
N	2.93494900	-2.00010100	-0.75224100
H	2.17779800	-1.31874400	-0.73533600
N	-4.04080500	1.38385200	-0.74299000
N	-3.92830900	-1.46428000	-0.67226400
C	4.41323200	0.55132900	-1.99258700
C	5.50273800	1.40230300	-1.99878000
H	6.46736900	1.19464500	-2.44061000
C	5.12298700	2.60216800	-1.33523800
H	5.74733300	3.47163400	-1.18312200
C	3.80734500	2.46491400	-0.93295100
C	2.86544600	3.44007100	-0.23140800
C	2.64460100	3.06464000	1.22845300
C	3.14272200	3.63291900	2.38600300
H	3.79256900	4.49531800	2.44090300
C	2.65388300	2.87723300	3.48660200
H	2.85790900	3.06590200	4.53132400
C	1.86201800	1.86022300	2.98579600
C	1.04923900	0.79397700	3.71024400
C	1.54927900	-0.62084500	3.44154500
C	2.09443700	-1.55745500	4.29987000
H	2.30384800	-1.40860800	5.34997000
C	2.31545800	-2.75209400	3.56108700
H	2.72704000	-3.67431000	3.94684500
C	1.90344000	-2.52977800	2.26059300
C	1.89510700	-3.45837500	1.05004200
C	3.00508400	-3.10710500	0.06806400
C	4.19341700	-3.74786300	-0.22712700
H	4.55327300	-4.65749700	0.23358200
C	4.84972600	-3.00158600	-1.24547700
H	5.79930000	-3.24277300	-1.70276200
C	4.05091000	-1.91786900	-1.55879400
C	4.21925800	-0.82777400	-2.60817300
C	3.50486100	4.84145800	-0.28570500
H	2.88868600	5.57581200	0.23980700
H	3.63112500	5.16059700	-1.32546700
H	4.48984300	4.83713400	0.18920400
C	1.13465300	1.06130700	5.22453800
H	0.53467500	0.32670900	5.77054500
H	0.75273400	2.06158000	5.45157600
H	2.16604000	0.99751400	5.58431700
C	-0.44276200	0.90494700	3.29604700
H	-0.59961700	0.73025700	2.22869200
H	-0.82094900	1.90760500	3.52938800
H	-1.03904900	0.16802600	3.84691800
C	2.10243000	-4.90181800	1.54547000
H	2.09386400	-5.60415000	0.70754600
H	1.30562300	-5.17688600	2.24386400
H	3.06027500	-5.00799700	2.06346000
C	2.97850200	-0.81032100	-3.54280500
H	2.04608900	-0.59119100	-3.01325900
H	2.86242600	-1.78789000	-4.02559900
H	3.10659700	-0.04893600	-4.32117100

C	5.45266600	-1.15910300	-3.46803800
H	5.58139300	-0.40392800	-4.24985000
H	5.32859200	-2.13691400	-3.94390100
H	6.36490700	-1.18582800	-2.86408300
C	1.52038600	3.45120900	-1.02607000
H	1.76451100	3.68667400	-2.07081800
H	1.10379700	2.44037800	-1.03741700
C	0.43772400	4.42287700	-0.54383800
H	0.15910500	4.21385400	0.49593000
H	0.83132000	5.44610300	-0.55667100
C	-0.81268400	4.41491200	-1.43454400
H	-1.33459300	5.37391500	-1.37303500
H	-0.52256100	4.29409800	-2.48800600
C	-3.09097300	3.61996400	-1.40464200
C	-4.18069500	2.70021400	-0.87218900
C	-5.37670300	3.39005800	-0.56235100
H	-5.41510400	4.45742700	-0.73499200
C	-6.42996300	2.68186800	-0.05122300
H	-7.35499800	3.17598000	0.23634500
C	-6.32322500	1.28374300	0.09147200
C	-5.10401300	0.65517300	-0.30299100
C	-5.03171600	-0.80722900	-0.23403700
C	-6.16431600	-1.51117600	0.28026800
C	-6.10679200	-2.91864200	0.33466300
H	-6.95723100	-3.46876100	0.73090200
C	-4.99070300	-3.56655400	-0.12309500
H	-4.88045400	-4.64324900	-0.12234000
C	-3.92154500	-2.79374600	-0.62749200
C	-2.73516100	-3.60802800	-1.12076300
C	-0.46699600	-3.61035900	-2.03384700
H	0.14471000	-2.83854000	-2.50497400
H	-0.71299000	-4.36795300	-2.78788300
C	0.31709700	-4.27322900	-0.88504500
H	1.29257900	-4.56179100	-1.29652400
H	-0.19566400	-5.19284800	-0.58921400
C	0.51054200	-3.35304500	0.33666700
H	-0.26907000	-3.54892600	1.08236400
H	0.36217100	-2.31696400	0.02407100
C	-7.42018300	0.52846400	0.61020200
H	-8.31614900	1.06326300	0.91481900
C	-7.33916300	-0.82146900	0.71135000
H	-8.16707400	-1.40680000	1.10331600
C	-0.27936300	0.07550200	-0.93217600
O	-0.56162100	-0.40222900	-2.03641600
O	-1.28583900	0.63034700	-0.16407000
O	0.86612200	0.12621700	-0.36496800
H	-2.15072900	0.48503900	-0.61206600
N	-1.80384000	3.39827600	-1.07348000
N	-1.69345900	-2.93373700	-1.62118300
H	-1.52650500	2.53887400	-0.60028600
H	-1.70807500	-1.91752000	-1.70127200

6. References

1. Ko, S.; Kim, S. K.; Share, A.; Lynch, V. M.; Park, J.; Namkung, W.; Rossom, W. V.; Busschaert, N.; Gale, P. A.; Sessler, J. L.; Shin, I. *Nat. Chem.* **2014**, *6*, 885-892.

2. He, Q.; Williams, N. J.; Oh, J. H.; Lynch, V. M.; Kim, S. K.; Moyer, B. A.; Sessler, J. L. *Angew. Chem., Int. Ed.* **2018**, *57*, 11924-11928.

3. Dolomanov, O.V., Bourhis, L.J., Gildea, R.J, Howard, J.A.K. & Puschmann, H. J. Appl. Cryst. 2009, 42, 339-341.

4. Sheldrick, G.M. Acta Cryst. 2015, A71, 3.

5. Sheldrick, G.M. Acta Cryst. 2015, C71, 3.

6. Gaussian 09, Revision **E.01**, Frisch, M. J.; Trucks, G. W.; Schlegel, H. B.; Scuseria, G. E.; Robb, M. A.; Cheeseman, J. R.; Scalmani, G.; Barone, V.; Petersson, G. A.; Nakatsuji, H.; Li, X.; Caricato, M.; Marenich, A. V.; Bloino, J.; Janesko, B. G.; Gomperts, R.; Mennucci, B.; Hratchian, H. P.; Ortiz, J. V.; Izmaylov, A. F.; Sonnenberg, J. L.; Williams-Young, D.; Ding, F.; Lipparini, F.; Egidi, F.; Goings, J.; Peng, B.; Petrone, A.; Henderson, T.; Ranasinghe, D.; Zakrzewski, V. G.; Gao, J.; Rega, N.; Zheng, G.; Liang, W.; Hada, M.; Ehara, M.; Toyota, K.; Fukuda, R.; Hasegawa, J.; Ishida, M.; Nakajima, T.; Honda, Y.; Kitao, O.; Nakai, H.; Vreven, T.; Throssell, K.; Montgomery, J. A., Jr.; Peralta, J. E.; Ogliaro, F.; Bearpark, M. J.; Heyd, J. J.; Brothers, E. N.; Kudin, K. N.; Staroverov, V. N.; Keith, T. A.; Kobayashi, R.; Normand, J.; Raghavachari, K.; Rendell, A. P.; Burant, J. C.; Iyengar, S. S.; Tomasi, J.; Cossi, M.; Millam, J. M.; Klene, M.; Adamo, C.; Cammi, R.; Ochterski, J. W.; Martin, R. L.; Morokuma, K.; Farkas, O.; Foresman, J. B.; Fox, D. J. Gaussian, Inc., Wallingford CT, **2009**.

7. Xu, X., Goddard, W. A. *Proc. Natl. Acad. Sci. USA* **2004**, *101*, 2673-2677.

8. Boys, S. F., Bernardi, F. *Mol. Phys.* **1970**, *19*, 553-566.

9. van Duijneveldt, F. B., van Duijneveldt-van de Rijdt, J. G. C. M., van Lenthe, J. H. *Chem. Rev.* **1994**, *94*, 1873-1885.